Microchimica Acta (2019) 186: 859
https://doi.org/10.1007/s00604-019-3904-9

REVIEW ARTICLE

Signal amplification in immunoassays by using noble metal nanoparticles: a review

Hualin Yang[1] · Wentao Xu[2] · Yu Zhou[1]

Received: 20 May 2019 / Accepted: 9 October 2019 / Published online: 30 November 2019

Abstract

This review (with 147 references) summarizes the state of the art in methods for signal amplification in immunoassays by using noble metal nanoparticles (MeNPs). Following an introduction into the field, a first large section covers MeNPs as signal tracers. The next sections describes the use of MeNPs as carriers for biomolecules, and of doped, decorated or functionalized MeNPs. A next large section covers MeNPs as used in aggregation-based assays that result in a change of color or dynamic light scattering (DLS). This is followed by a discussion of MeNPs that undergo etching, size reduction, or growth and thereby change color and DLS, with subsections on methods based on etching, particle growth or particle formation. We then rview methods where MeNPs acts as catalysts (enzyme mimics), with subsections on MeNPs and on doped or composed MeNPs. A final large section discusses the synergies of MeNPs or multiple signal amplification strategies in immunoassays. Several Tables are presented that give an overview on the wealth of methods and materials. A concluding section summarizes the current status, addresses current challenges, and gives an outlook on potential future trends.

Keywords Noble metal nanoparticles · Signal amplification · Nano materials · Immuno sensors

Introduction

The sensitivity of any immunoassay is determined mainly by the intensity of the output signal. As the increasing demands for environmental monitoring [1], food safety analysis [2], disease diagnosis [3] and other research areas [4–6], novel signal amplification strategies are required to maximize the signal output. A variety of metal nanoparticles (NPs), or metal NPs doped by other materials have nontoxicity, chemical stability, fine biological compatibility, excellent catalytic activity and high surface-to-volume ratio. They have been widely used as essential components of signal amplification strategies to enhance the sensitivity of the immunoassays. They include magnetic bead [7], gold NPs (AuNPs) [8], silver NPs (AgNPs) [9], Fe_3O_4@SiO_2 [4], Ag@bovine serum albumin (Ag@BSA) [10], zinc oxide nanoflower-bismuth sulfide composites (ZNF@Bi_2S_3) [11] and so on. With the development of nanotechnology, great attention has been paid to the combination of different nanomaterials to develop the signal amplification strategies. These strategies include magnetic NPs/aptamer/carbon dots nanocomposites [12], TiO_2/S-$BiVO_4$@Ag_2S nanocomposites [13], MoS_2-PEI-Au nanocomposites and Au@BSA core/shell NPs [14], N-GNRs-Fe-MOFs@AuNPs nanocomposites and AuPt-methylene nanorod [15]. Metal NPs with rich nanostructures not only load large number of signal elements such as antibody and enzyme, but also improve the electronic properties and produce detectable signals for indirect detection of targets, resulting high sensitivity of an immunoassay. Several reviews have been published focused on the synthesis, performance and applications of metal NPs in assay design [16–22], few dedicated to the signal amplification strategies in immunoassays. Here, we summarize selected articles from 2007 onwards on noble metal NPs as elements of signal amplification strategies in the development of immunoassays. Various signal amplification strategies using noble metal NPs are summarized in Fig. 1, such as serving as (a) signal tracers, (b) carriers, (c)

✉ Wentao Xu
xuwentao@cau.edu.cn

✉ Yu Zhou
zhouyurunye@sina.com

[1] College of Animal Sciences/ College of Life Science, Yangtze University, Jingzhou 434023, People's Republic of China

[2] Beijing Advanced Innovation Center for Food Nutrition and Human Health, College of Food Science & Nutritional Engineering, China Agricultural University, Beijing 100083, People's Republic of China

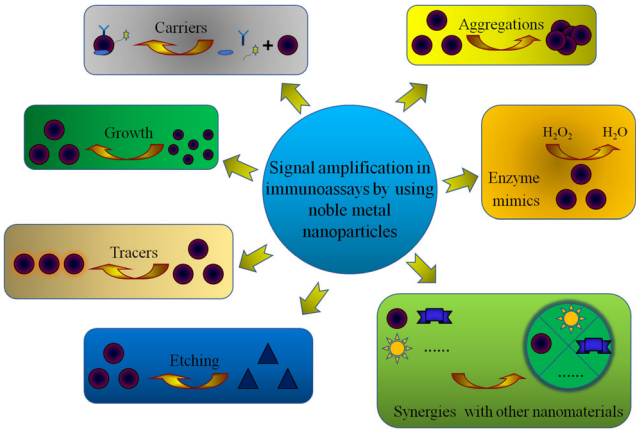

Fig. 1 The roles of metal NPs in signal amplification in immunoassays

aggregators, (d) enzyme mimics, (e) in growth or etching of NPs, and (f) in synergistic effects.

Noble metal NPs serving as signal tracers

Gold nanoparticles (AuNPs) have the distinguishing physical and chemical properties, such as biocompatibility, easy conjugation to biomolecules and better electrochemical or optical transduction property. They have become highly valuable nanomaterials in signal amplification strategies of immunoassay **(**Table 1**)**. AuNPs labeled with antibody can act as the tracers for signal amplification by increasing amount of themselves in the position of detection line. Without any complicated labeling procedure, positively charged AuNPs-tracers can be directly bound to the negatively charged antibodies. Based on this mechanism, a large number of lateral flow assays utilizing antibody labeled positively charged AuNPs have been designed for different targets [23–26]. The AuNPs act as signal amplification tracers accumulate numerous AuNPs on test line which are correlated with the amounts of target in samples.

To further enhance the sensitivity, an AuNPs growth and accumulation signal amplification strategy based lateral flow assay was developed for rapid detection of Salmonella Enteritidis [27]. For having high catalytic activity, AuNPs produce new AuNPs on the surface of the initial AuNPs during the reaction between $HAuCl_4$ and $NH_2OH{\cdot}HCl$. The remarkable enhanced signal can be clearly and visually distinguished even under a lower concentration of S. Enteritidis. The sensitivity (10^4 CFU/mL) is enhanced 100-fold compared to the traditional AuNPs based strategy (10^6 CFU/mL). This AuNPs growth and accumulation signal amplification strategy based assay need two "10 min reaction" steps (Fig. 2**a**).

For signal amplification of lateral flow assay without an additional operation step, a strategy utilizing two AuNP-antibody conjugates was designed for detection of troponin I [28]. The 1st AuNPs-tracer was the AuNPs labeled with an anti-troponin I antibody and the 2nd AuNPs-tracer was the AuNPs labeled with an anti-BSA antibody. The 2nd AuNPs-tracer was designed to bind only with the 1st AuNPs-tracer with a higher size. Both two AuNPs-tracers act as signal amplification probes to aggregate numerous AuNPs on test line. The detection sensitivity (0.01 ng/mL) is increased about 100-fold compared to the conventional lateral flow assay (1 ng/mL) (Fig. 2**b**). Fang and coworkers designed a dual labeling signal amplification strategy using high affinity AuNPs-biotinylated anti-pesticide imidacloprid antibody (nanogold-BAb) and nanogold-streptavidin (nanogold-Sa) probe (Fig. 2**c**). The detection signal was the amount of nanogold-BAb and nanogold-Sa probes. The signal amplification was achieved by using nanogold-BAb probe for the determination of imidacloprid and nanogold-Sa probe for signal enhancement. The visual detection sensitivity and semi-quantitative analytical capacity of the assay are 10-fold and 160-fold higher than those of traditional lateral flow assay, respectively [29]. The immunochromatographic assays based on metal nanomaterials as signal tracers are simple, rapid and convenient to perform, and no equipments and professional

Table 1 An overview on metal nanomaterials commonly used as signal tracers in immunochromatographic assays

Particle type	Principle	Targets	Limit of detection	Measurement range	Reference
AuNPs[1]	Accumulation	Carbohydrate antigen	5 U/mL	5-100 U/mL	[23]
AuNPs	Accumulation	*Streptococcus agalactiae*	1.5×10^5 CFU	N [3]	[25]
AuNCs[2]	Quenching	Cadmium ions	0.18 ng/mL	0.25-8 ng/mL	[24]
AuNPs	Growth and accumulation	Salmonella Enteritidis	10^4 CFU/mL	10^3-10^8 CFU/mL	[27]
AuNPs	Dual AuNPs accumulation	Troponin I	0.01 ng/mL	0.10-14.27 ng/mL	[28]
AuNPs	Loop-mediated isothermal amplification	*E. coli* O157:H7	1 cell	1-10^5 cells	[26]

[1] Nanoparticles; [2] Nanoclusters; [3] Not provided;

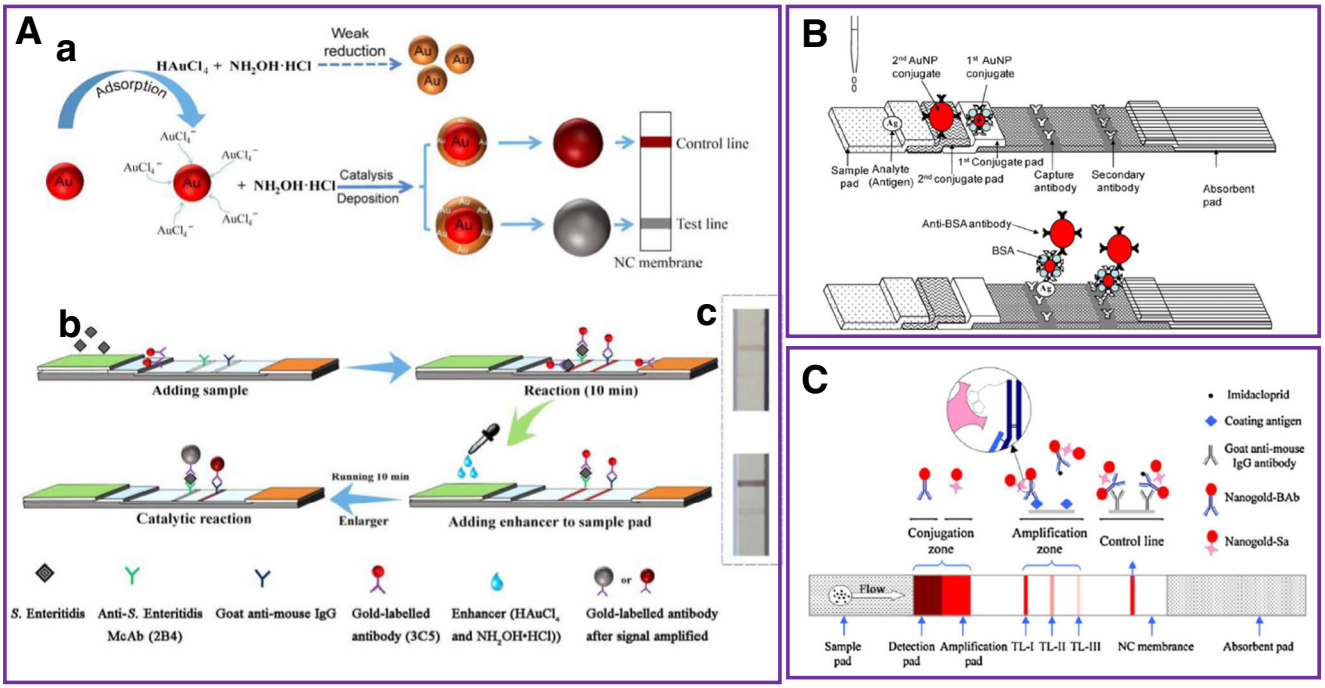

Fig. 2 Schematic diagram of metal NPs themselves as signal tracers. (A) AuNPs growth and accumulation signal amplification strategy based lateral flow assay. (a) principle of the signal amplification, (b) analysis process of the signal amplified lateral flow assay, (c) comparison pictures for enhancement effect illustration. Reproduced with permission from Ref. [27]. Copyright Elsevier, 2017. (B) Schematic illustration of the dual AuNPs-tracers based lateral flow assay. Reproduced with permission from Ref. [28]. Copyright Elsevier, 2010. (C) Schematic illustration of the dual labeling signal amplification strategy based lateral flow assay. Reproduced with permission from Ref. [29]. Copyright Elsevier, 2015

analyst are required. Meanwhile, the sensitivities of these techniques are relatively lower compared to other assays.

Noble metal NPs serving as carriers

Noble metal NPs themselves as carriers for antibody, enzyme and other bio-molecules

Various material NPs, such as AuNPs, TiO_2, as well as CuS-SiO_2 have high surface areas, unique physicochemical properties, high chemical stability and ease to be functionalized. They have been used as carriers for loading different signal elements including antibodies, enzymes, oligo nucleotides and other bio-molecules [5, 7, 30–43] (Table 2).

Based on sandwich immunoreactions, AuNPs were used as labeling carriers of horseradish peroxidase (HRP)-antibody in combination with TMB as substrates. Parolo and coworkers designed a lateral flow format for detection of Human IgG used as model protein [44]. AuNPs have high surface areas of AuNPs, which load more amount of HRP than that of IgG. The signal amplification of catalytically oxidized substrate related to the concentration of targets is enhanced around 10-fold compared to the results that obtained just from the direct measurement of the AuNPs as non-modified tracers. Zhou's group used AuNPs as carriers for loading antibody and HRP simultaneously, and developed a competitive immunoreaction format for detection of Pb(II) [45]. As low as 9 pg/mL of Pb(II) is still detectable, while for traditional IgG-HRP based ELISA only signal as high as 750 pg/mL of target is distinguishable [45]. Yin et al. designed an electrochemical immunoassay by using AuNPs as carrier for loading anti-His tag antibody labeled with HRP as signal amplification unit and methyl binding domain protein of MeCP2 as DNA CpG methylation recognization unit (Fig. 3**a**). After an immunoreaction, the AuNPs-IgG-HRP was captured on the electrode surface. Under the catalysis of HRP towards hydroquinone oxidized in the presence of H_2O_2, the amplified electrochemical reduction signal was produced [46].

On the basis of competitive immunoassay, Wang's group proposed a bio-barcode amplification strategy for detection of small molecules, triazophos. In the assay, AuNPs were used as carrier for loading 6-carboxyfluorescein labeled single-stranded thiol-oligonucleotides and antibody. The targets in the sample compete with ovalbumin (OVA)-haptens coated on the bottom of microplate for binding to the antibody-AuNP-thiol-oligonucleotides. The fluorescence intensity quenched by AuNPs was inversely proportional to concentration of triazophos (Fig. 3**b**). The prominent advantage of the competitive fluorescence bio-barcode immunoassay is higher sensitivity than indirect competitive ELISA [13].

Table 2 Summary of the applications of metal NPs used as carriers in immunoassays

Particle type	Principle of signal output	Targets	Limit of detection	Measurement range	Reference
AuNPs[1]	Chemiluminescent	Carbohydrate antigen	0.016 U/mL	0.025-1.00 U/mL	[32]
AuNPs	Electrochemical immunosensor	M. SssI	0.017 unit/mL	0.05-90 unit/mL	[46]
AuNPs@ PAMAM/MWCNT@Chi nanocomposite	Electrochemical impedance immunosensor	Salmonella typhimurium	5-10^2 U/mL	1.0×10^3 - 1.0×10^7 U/mL	[53]
AuNPs@BSA/ luminol/MoS_2- polyethylenimine	Electrochemiluminescence	α-fetoprotein	1.0×10^5 ng/mL	0.0001-200.0 ng/mL	[63]
AuNPs@MWCNTs	Electrochemical immunosensor	Carcinoembryonic antigen and a-fetoprotein	3.0 pg/mL and 4.5 pg/mL	0.01-60 ng/mL	[55]
AuNPs@6-carboxyfluorescein	Fluorescence bio-barcode	Triazophos	6 ng/mL	0.01-20 ng/mL	[13]
Fe_3O_4	On-chip electrochemical sensor	β-hCG	10 mIU/mL	N [a]	[64]
Fe_3O_4	Electrochemiluminescence	Prostate-specific antigen	0.8 pg/mL	0.003-20 ng/mL	[37]
AuNPs/Fe_3O_4	Nano-ELISA	Protein p53	5 pg/mL	N [2]	[30]
AuNPs@SiO_2	Chemiluminescent	α-fetoprotein	0.005 ng/mL	0.01-0.5 ng/mL	[62]
AuNPs@γ-Fe_2O_3	Surface-enhanced Raman spectroscopy	Carcinoembryonic antigen	0.1 ng/mL	1-50 ng/mL	[34]
AuNPs@mesoporous silica/ toluidine blue	Electrochemical immunosensor	α-fetoprotein	0.05 pg/mL	10^{-4}-10^3 ng/mL	[51]
Fe_3O_4@graphene nanosheets	Electrochemiluminescence	Prostate specific antigen	0.72 pg/mL	0.003-50 ng/mL	[35]
Fe_3O_4@SiO_2	Electrochemiluminescence immunosensor	5-hydroxymethylcytosine	0.047 nM	0.1-30 nM	[4]
AuNPs@AgPt	Amperometric immunosensor	Zearalenone	1.7 pg/mL	0.005-15 ng/mL	[52]
Luminol-AgNPs@ mesoporous carbon	Electrochemiluminescence	Aflatoxin B1	50 fg/mL	0.1 pg/ mL −50 ng/mL	[54]
Ferrocene@ZnONRs	Electrochemical immunoassay	E. coli	50 cfu/mL	10^2-10^6 cfu/mL	[47]
Ru@SiO_2	Photoelectrochemical immunosensor	N^6-methyladenosine	3.23 pM	0.01-10 nM	[12]
CuS@SiO_2 + Carbon@TiO_2/CdS	Photoelectrochemical immunosensor	Insulin	0.03 pg/mL	0.1 pg/ mL −50 ng/mL	[65]
TiO_2NPs	Chemiluminescent	Human IgG	0.1 ng/mL	0.5-200 ng/mL	[31]

[1] Nanoparticles; [2] Not provided;

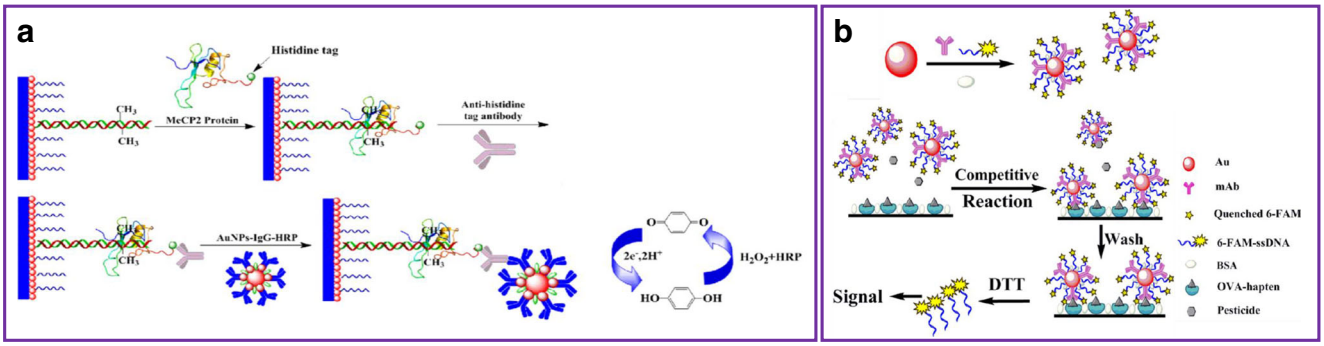

Fig. 3 Schematic diagram of metal NPs as carriers. **a** AuNPs as carrier for loading antibody, HRP and methyl binding domain protein of MeCP2 in electrochemical immunoassay. Reproduced with permission from Ref. [46]. Copyright Elsevier, 2013. **b** AuNPs as carrier for loading antibody and 6-carboxyfluorescein labeled single-stranded thiol-oligonucleotides in competitive fluorescence bio-barcode immunoassay. Reproduced with permission from Ref. [13]. Copyright Elsevier, 2017

Noble metal NPs doped, decorated or functionalized with other materials as carriers or signal labels

To further enhance the sensitivity of immunoassays, metal NPs integrated with other materials have been employed as carriers to design various signal amplification strategies [47–61]. For example, using thionine (TH)-doped mesoporous ZnO nanostrawberries (MP-ZnO) for loading HRP labeled goat anti-human IgG (HRP-anti-IgG), and the immobilized ultralong Ag nanowires with the capture antibody (Fig. 4**a**), Cao et al. developed an electrochemical immunoassay for detection of human IgG [48]. The electrochemical signal of the sandwich-type immunoassay was significantly amplified due to crystalline framework, high surface area of the MP nanomaterials and the superconductivity of silver nanowires.

Based on zinc oxide nanoflower-bismuth sulfide (ZNF@Bi_2S_3) composites materials and reduced graphene oxide (rGO), a photoelectrochemical (PEC) immunoassay was constructed for squamous cell carcinoma antigen (SCCA) detection [11]. In the assay, ZNF@Bi_2S_3 composites and rGO were used as photoactive materials and signal labels respectively. HRP was used not only to block nonspecific binding sites, but also participate in luminol-based chemiluminescence (CL) system to induce inner light source. The induced CL emission acted as an inner light source excited photoactive materials. The rGO trigged the CL resonance energy transfer between luminol and rGO which decreased the efficient of CL emission to ZNF@Bi_2S_3 composites and electrons amount to electrode surface. The steric hindrance, increased by the introduced rGO-Ab_2 hindered the electron donor to the surface of Bi_2S_3 for reaction with the photogenerated holes (Fig. 4**b**). This novel signal amplification strategy based PEC immunoassay exhibits low detection limit, good reproducibility and wide linear ranges. Based on avidin functionalized Ru@SiO_2 and carboxylated g-C_3N_4(CN), Ai and Yin's group constructed another PEC immunoassay [12]. In the assay, N_6-methyladenosine-5′-triphosphate (m6ATP), Ru@SiO_2 and CN were used as the detection target molecule, signal amplification unit to improve the photocurrent and the support for the antibody immobilization, respectively. Phos-tag-biotin was employed as bridge of target and Ru@SiO_2 (Fig. 4**c**). The sensitivity of the PEC immunoassay is improved by the specific interaction between Phos-tag and phosphate group, biotin and avidin.

Metal NPs have been doped with other materials, such as AuNP-doped BSA microspheres (Au@BSA) [14], nanosilver-doped BSA microspheres (Ag@BSA) [10] and AuNP-doped mesoporous SiO_2 (Au/SiO_2) [62]. They can be employed as carrier for loading numerous molecule recognition antibody, HRP or luminol molecules in electrochemical immunoassays. For example, Zhang and coworkers developed a sandwich-type electrochemiluminescence immunoassay for the detection of alpha fetal protein (AFP) by using luminol-Au@BSA NPs to load secondary antibodies (Ab_2) and luminol molecules [14]. In the assay, the MoS_2 nanosheets were labeled with polyethylenimine (PEI) polymer and AuNPs were electrostatically adsorbed to form MoS_2-PEI-Au nanostructures. The target molecules were sandwiching captured by the primary antibody (Ab_1) and the luminol-Au@BSA-Ab_2 nanocomposite through specific immunoreactions (Fig. 4**d**). The electrochemiluminescence signal amplification was achieved by the catalytic performance of MoS_2-PEI-Au nanocomposites. Zhou and coworkers assembled a HRP-tyramine conjugates electrochemical immunoassay based on nanosilver-doped BSA microspheres (Ag@BSA) and glassy carbon electrode for detection of carcinoembryonic antigen (CEA). HRP and detection antibody were immobilized on the surface of Ag@BSA (Fig. 4**e**). The signal amplification was obtained by coupling enzymatic biocatalytic precipitation with tyramine and carbon electrode modified with capture antibody [10]. The multi-enzyme assembly electrochemical immunoassay exhibits higher sensitivity in comparison with traditional Ag@BSA labeling method.

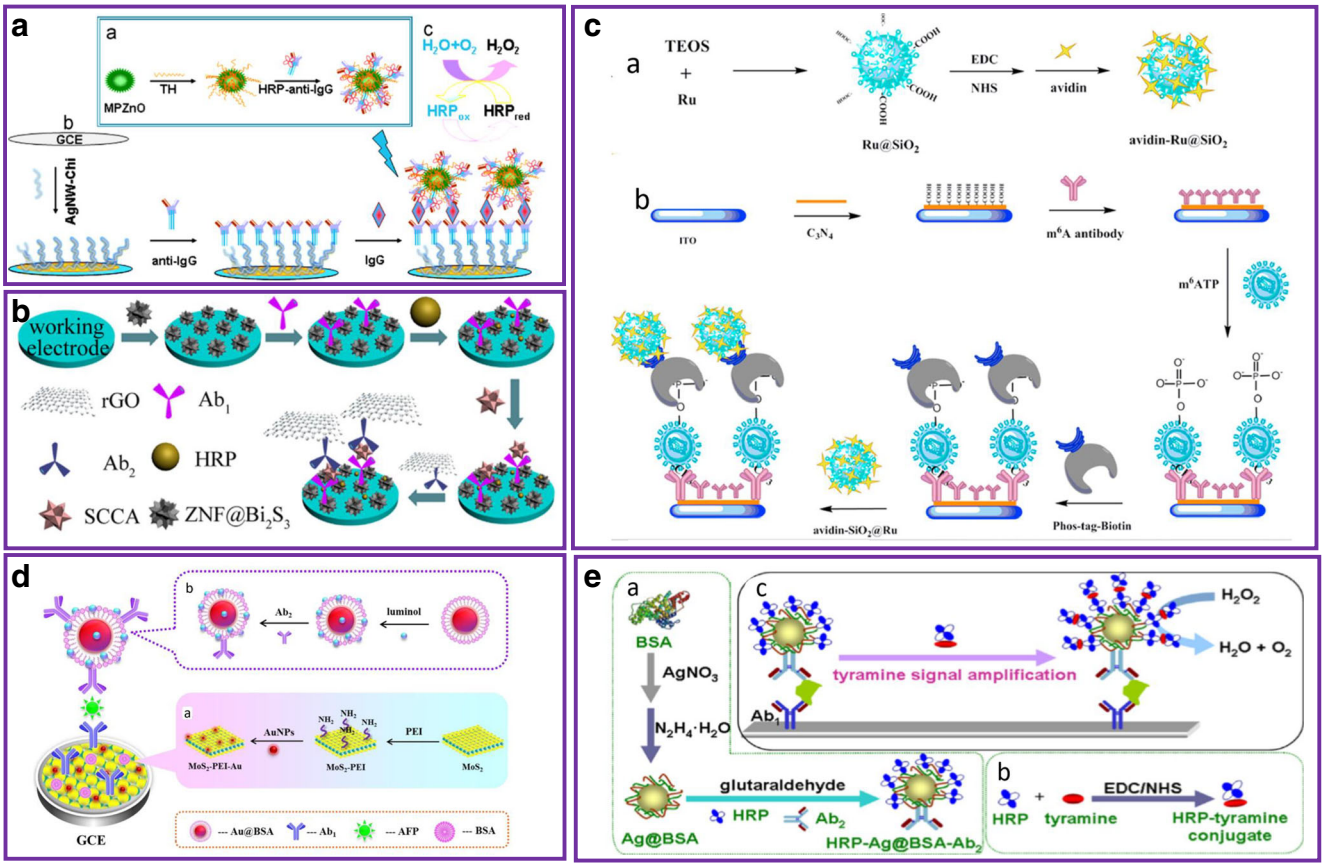

Fig. 4 Schematic diagram of metal NPs doped or functionalized with other materials as carriers. (A) MP-ZnO functionalized with TH as carrier for loading HRP-anti-IgG in electrochemical immunoassay. (a) preparation procedure of MP-ZnO-TH for loading HRP-anti-IgG, (b) schematic view of electrochemical sandwich-type electrochemical immunoassay procedure. Reproduced with permission from Ref. [48]. Copyright Elsevier, 2013. (B) ZNF@Bi_2S_3 composites as carrier for loading capture antibodies in photoelectrochemical (PEC) immunoassay. Reproduced with permission from Ref. [11]. Copyright Elsevier, 2015. (C) Avidin functionalized Ru@SiO_2 as signal labels in PEC immunoassay. (a) preparation procedure of avidin functionalized Ru@SiO_2, (b) schematic view of PEC immunoassay procedure. Reproduced with permission. Reproduced with permission from Ref. [12]. Copyright Elsevier, 2018. (D) Au@BSA functionalized with luminol as carrier for loading Ab_2 in electrochemiluminescence immunoassay. (a) formation of MoS_2-PEI-Au nanocomposites, (b) preparation procedure of luminol-Au@BSA-Ab_2 cojugation. Reproduced with permission from Ref. [14]. Copyright Elsevier, 2017. (E) Ag@BSA functionalized with HRP and Ab_2 as carrier for loading tyramine in multi-enzyme assembly electrochemical immunoassay. (a) preparation procedure of HRP-Ag@BSA-Ab_2, (b) schematic view of HRP-tyramine conjugate, (c) schematic view of multi-enzyme assembly electrochemical immunoassay. Reproduced with permission from Ref. [10]. Copyright Elsevier, 2013

The sensitivities of these methods were improved by employing metal NPs as bio-molecules carrier because the metal NPs offer an opportunity to load a large amount of biomolecules, such as enzymes improving the sensitivity of the assay. However, the stability of metal NPs based probes in immunoassays are comparable lower than those of IgG-enzyme conjugates. And the synthesis procedures of metal NPs probe are time-consuming and labor-intensive. Table 2 summarizes the main characteristics of these methods.

Noble metal NPs serving as aggregations

Localized surface plasmon resonance (LSPR) is the most remarkable inherent optical properties of AuNPs and AgNPs. Colloidal solutions of AuNPs and AgNPs have different colour in the visible spectrum region when they are well spaced in comparison with when they are aggregated. Therefore, designed immunoreactions between the analyte and the metal NPs can lead to a colour change of the solution. The aggregations of AuNPs and AgNPs change the colour of colloidal solution from red to purple-blue and from yellow to brown respectively allowing the visual detection of the target analyte [21] (Table 3).

Noble metal NPs as aggregations induced by addition of target analyte to trigger the change of colour and DLS of the solution

Based on aggregation of antibody-functionalized NPs coupled with DLS, sandwich type format (NPs-Ab_1-analyte-Ab_2-NPs) metal NPs aggregation assays (NanoDLSays) are used as a

Table 3 An overview on metal nanomaterials commonly used as aggregations in immunoassays

Particle type	Principle	Analytical application	Limit of detection	Measurement range	Reference
AuNPs [1]	Dynamic light scattering	Protein	5 μg/mL	10-25 μg/mL	[66]
AuNPs	Dynamic light scattering	Human IgG	10 ng/mL	0.05-10 μg/mL	[67]
AuNPs	Colorimetric method	Casein	0.03 μg/mL	0.08-250 μg/mL	[68]
AuNPs	Enzyme-mediated surface plasmon resonance	Treponema pallidum	0.98 pg/mL	1 pg/ mL-10 ng/mL	[72]
AgNPs	Dynamic light scattering	Hepatitis B surface antigen	0.005 IU/mL	0.005-1 IU/mL	[70]
AuNPs	DNA nano-assembly protection	ATP	0.75 μM	N [2]	[73]
Au@AgNPs	Colorimetric and surface enhanced Raman scattering	Alkaline phosphatase activity	0.1 U/L	0.50-10.0 U/L	[74]

[1] Nanoparticles; [2] Not provided;

model to establish the general immunoassays in the fields of molecular biology [66, 67], food analysis [68] and clinical diagnostics [69, 70]. Zhou's group proposed a NanoDLSay by using functionalized AuNPs with anti-β-casein mono- (McAb) and polyclonal (PcAb) antibodies, respectively as probes for detection of β-casein in bovine milk [68]. After addition of sample to the AuNPs probes, aggregation of AuNPs occurred through sandwich type format immunoreactions. The β-casein triggered AuNPs aggregation resulted in an obvious colour change from red to blue which

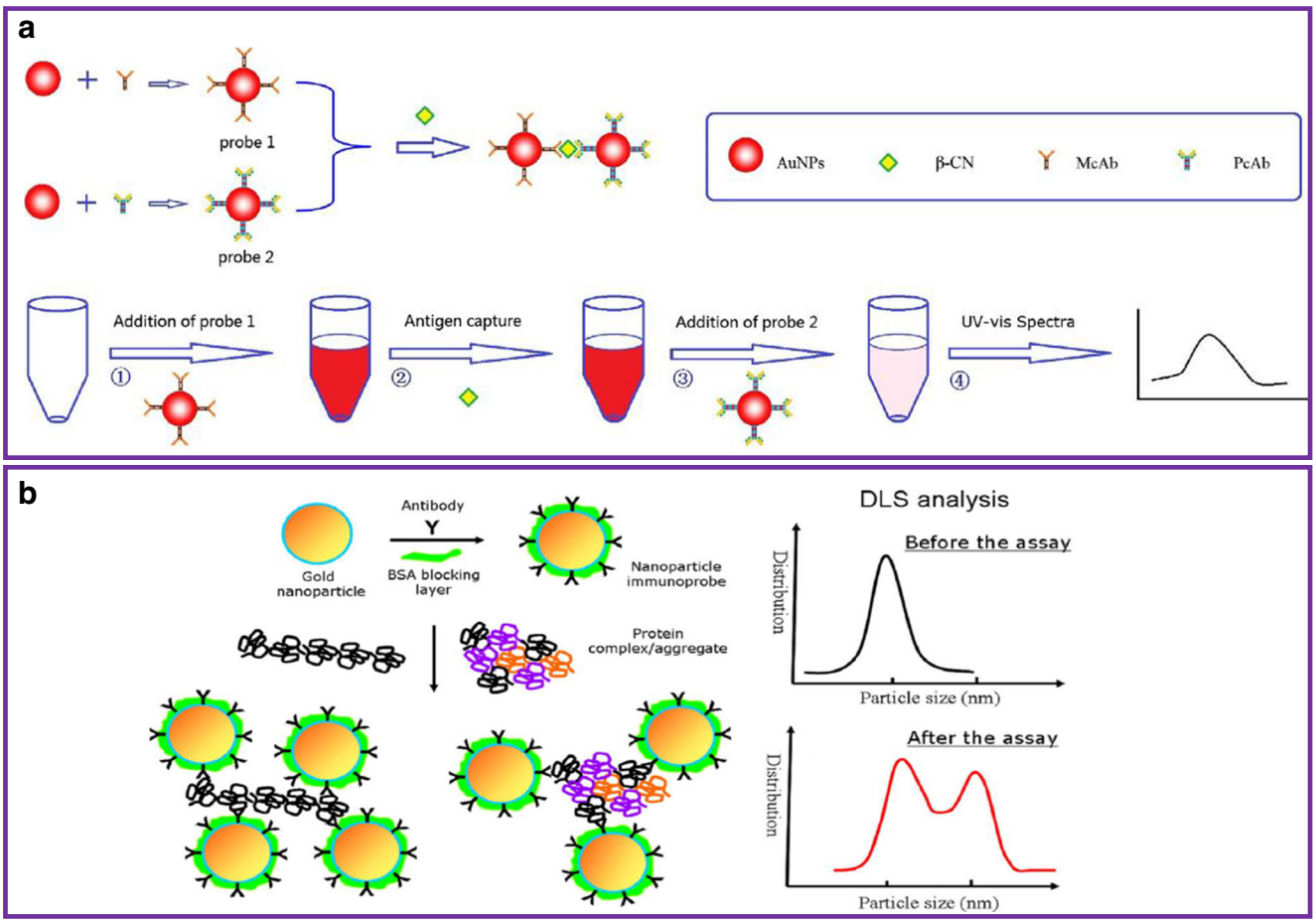

Fig. 5 Schematic diagram of AuNPs as aggregations induced by target analyte. **a** Schematic diagram of AuNPs functionalized by anti-β-casein McAb and PcAb, respectively as probes in NanoDLSay. Reproduced with permission from Ref. [68]. Copyright Elsevier, 2014. **b** Schematic diagram of AuNPs functionalized by anti-PAP McAb as aggregations in NanoDLSay. Reproduced with permission from Ref. [69]. Copyright Elsevier, 2010

was also monitored with DLS (Fig. 5**a**). Huo designed a NanoDLSay by using anti-prostatic acid phosphatase (PAP) McAb labeled with AuNPs as probes for examine of PAP (Fig. 5**b**), a potential biomarker for prostate cancer detection and diagnosis [69].

Noble metal NPs as aggregations induced by enzyme to trigger the change of colour and DLS of the solution

Enzyme-mediated aggregation of AuNPs in plasmonic ELISA (P-ELISA) has received considerable attention because it allows a naked-eye detection of target in very low numbers. Based on HRP-mediated AuNPs aggregation, Xiong's group integrated a P-ELISA for highly sensitive detection of ochratoxin A (OTA) [71]. In this assay, anti-OTA McAb was used as a coating antibody and OTA-labeled catalase (CAT) conjugate (OTA-CAT) was used as competing antigen to consume H_2O_2. AuNPs aggregation was triggered through the phenol polymerization of tyramine (TYR), which was induced by hydroxyl radicals from HRP-catalyzed H_2O_2. The color response generated through AuNPs aggregation (Fig. 6**a**). The signal output was amplified by ultrahigh CAT catalytic activity for H_2O_2. The designed P-ELISA exhibit a high sensitivity for OTA quantitation with a cut-off limit of 150 pg/mL visually. Based on acetylcholinesterase (AChE)-mediated aggregation of AuNPs, Nie and coworkers developed an ultrasensitive P-ELISA for the detection of total antibodies to *T. pallidum* [72]. The immunoreactions of the target antibodies were triggered by the AChE-catalyzed hydrolysis of acetylthiocholine to produce thiocholine which changed the surface charge distribution on the AuNPs and lead to the agglomeration of the AuNPs (Fig. 6**b**). The induced changes of DLS allowed the quantitative assay of *T. pallidum* antibodies. The sensitivity (0.89×10^{-12} g/ml) is 1000-fold improvements in sensitivity over a conventional ELISA (1.0×10^{-9} g/ml).

The major limitation of the aggregations based immunoassays is 'autoaggregation'. external factors, such as pH, ionic strength and temperature may induce undesirable aggregation of metal nanoparticles, and then result in high backgrounds or false positive results.

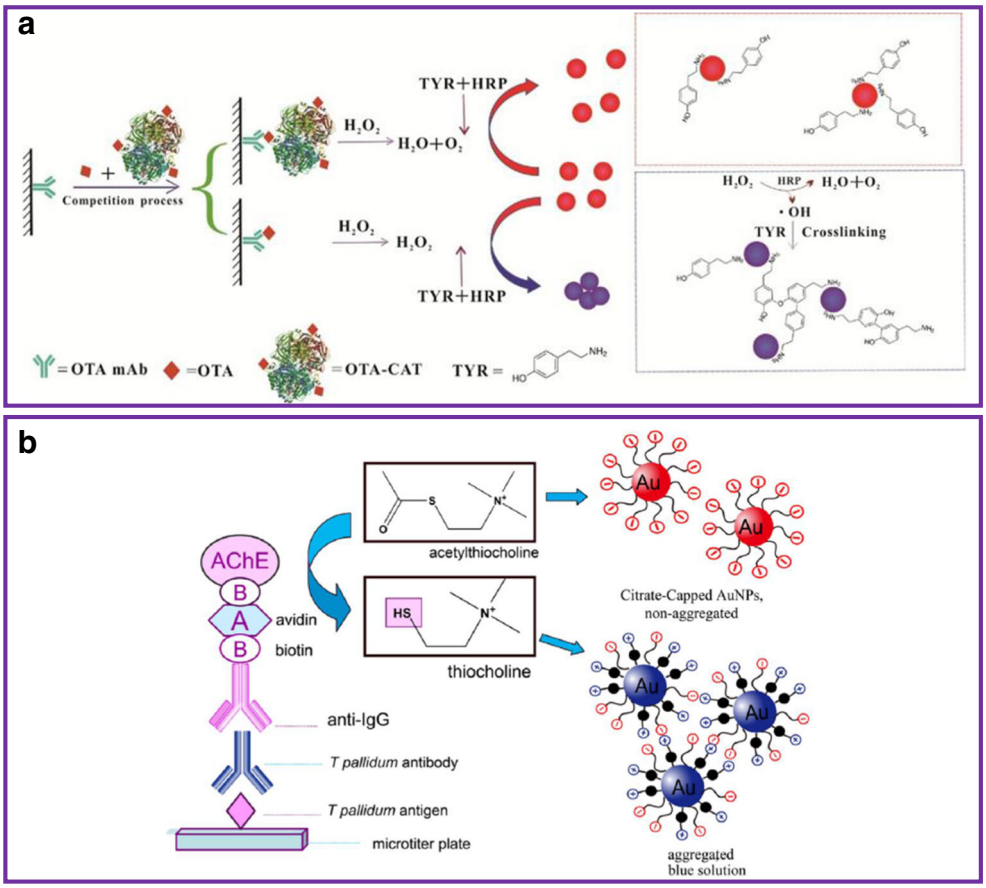

Fig. 6 Schematic diagram of enzyme-mediated aggregation of AuNPs in P-ELISA. **a** Schematic diagram of HRP-mediated AuNPs aggregation for detection of OTA. Reproduced with permission from Ref. [71]. Copyright Elsevier, 2017. **b** Schematic diagram of AChE-mediated aggregation of AuNPs for detection of anti-*T. pallidum* antibodies. Reproduced with permission from Ref. [72]. Copyright Elsevier, 2014

Noble metal NPs serving as in etching or growth of NPs

The LSPR extinction of AuNPs and AgNPs is strongly dependent upon the diameter, morphology, composition, the surrounding media, and aggregation state of the NPs [16]. Through mediated etching or growth of the NPs, enhanced signal amplification linearly correlated with the concentrations of analytes can be achieved [73, 75, 76] **(**Table 4**)**.

Noble metal NPs by etching to change the colour and DLS of the solution

Based on alkaline phosphatase (ALP)-triggered etching of gold nanorods (AuNRs), Zhang and coworkers designed a P-ELISA for highly sensitive colorimetric detection of human IgG [55]. As the sandwich-type immunocomplex formation reaction, the ALP labeled on the antibody hydrolyzed ascorbic acid 2-phosphate into ascorbic acid. Subsequently, iodate was reduced to iodine which etched AuNRs from rod to sphere in shape, leading to a blue-shift of LSPR (Fig. 7**a**). The visual P-ELISA achieved a naked-eye detectable limit of 3 ng/mL of human IgG. Based on CAT-triggered etching of triangular silver nanoprisms (AgNPRs), Yao and coworkers designed an AgNPRs etching P-ELISA for colorimetric determination of Cr (III) in environmental water samples. H_2O_2 was used to etch triangular AgNPRs into spherical AgNPRs, inducing a change in color and the LSPR wavelength shift of the AgNPRs reaction solution. The reaction was achieved by controlling H_2O_2 concentration that remains after degradation by CAT which was labeled with an Ab_2. The color change and the LSPR wavelength shift were closely correlated with the concentration of Cr (III). The developed P-ELISA can be used for the quantitative detection of Cr (III) with a limit of detection (LOD) of 3.13 ng/mL through the LSPR wavelength shift of the solution. They also can be used for the visual detection of Cr (III) with a sensitivity of 6.25 ng/mL indicated by a color visual change [77]. Also based on AgNPRs etching principle, Tang's group proposed a glucose oxidase (GOx)-triggered P-ELISA for the detection of cancer biomarkers [78]. In the assay, GOx catalysed oxidation of glucose to produce H_2O_2 which acted as an oxidant to etch the AgNPRs into smaller spherical silver NPs (Fig. 7**b**). The reaction was accompanied by substantial blue shift of the LSPR and change of colour of the solution. The AgNPRs-etched P-ELISA can be used for the detection of cancer biomarkers in the concentrations from 10 fg/mL to 100 pg/mL.

Noble metal NPs by growth to change the colour and DLS of the solution

Based on ALP-mediated growth of AgNPs, Xuan and coworkers developed a visual P-ELISA for sensitive and rapid detection of cancer biomarkers in clinical serum samples [79]. In the assay, ALP was bound to the detection antibody and the AgNPs were integrated with ALP, which hydrolyzed ascorbic acid-phosphate to produce reductant ascorbic acid. Subsequently, the ascorbic acid reacted with silver ions to produce metal silver which nucleated to become silver nanocrystals. The further growth of silver nanocrystals resulted in the formation of larger sized AgNPs (Fig. 8**a**). As a consequence, the colorless solution turned yellow along with the appearance of an absorption band at around 400 nm. The color intensity of the solution as well as their corresponding absorbance was proportional to the concentrations of analytes. Based on GOx-catalyzed growth of AuNPs, Liu and coworkers described a quantitative colorimetric immunoassay for ultrasensitive detection of cancer biomarkers [80]. The surfaces of magnetic beads (MBs) were modified with detection antibody (Ab_2) labeled by GOx which can generate H_2O_2. After a sandwich immunoreaction on the polystyrene substrate, the captured target pulled down the Ab_2-GOx-MBs conjugates on the substrate, where the GOx catalyzed the oxidation of glucose to produce H_2O_2. The produced H_2O_2 lead the growth of AuNPs in the presence of $AuCl_4^-$, resulting the colour and DLS changes of the solution (Fig. 8**b**).

Table 4 An overview on the etching and growth of metal NPs in immunoassays

Particle type	Principle	Targets	Limit of detection	Measurement range	Reference
AuNPs [1]	Catalase-catalyzed growth	Prostate specific antigen	1.0×10^{-18} g/mL	N [a]	[75]
AuNPs	EDTA-mediated growth	Cancer antigen	7.5×10^{-15} U/mL	$0.4\text{-}10 \times 10^{-12}$ U/mL	[81]
AuNPs	Glucose oxidase -catalyzed growth	Cancer biomarkers	93 aM	$10\text{-}10^5$ fg/mL	[80]
AgNPRs [2]	Glucose oxidase-mediated Etching	Prostate specific antigen	4.1 fg/mL	10 fg/mL-100 pg/mL	[78]
AgNPs	Alkaline phosphatase -mediated growth	Cancer biomarkers	0.23 ng/mL	N [3]	[79]
AgNPRs	Catalase-mediated Etching	Cr(III)	3.13 ng/mL	3.13-50 ng/mL	[77]
AuNPs	Iodine-Mediated Etching	Human IgG	100 pg/mL	0.1-10 ng/ mL	[55]

[1] Nanoparticles; [2] Nanoprism [3] Not provided;

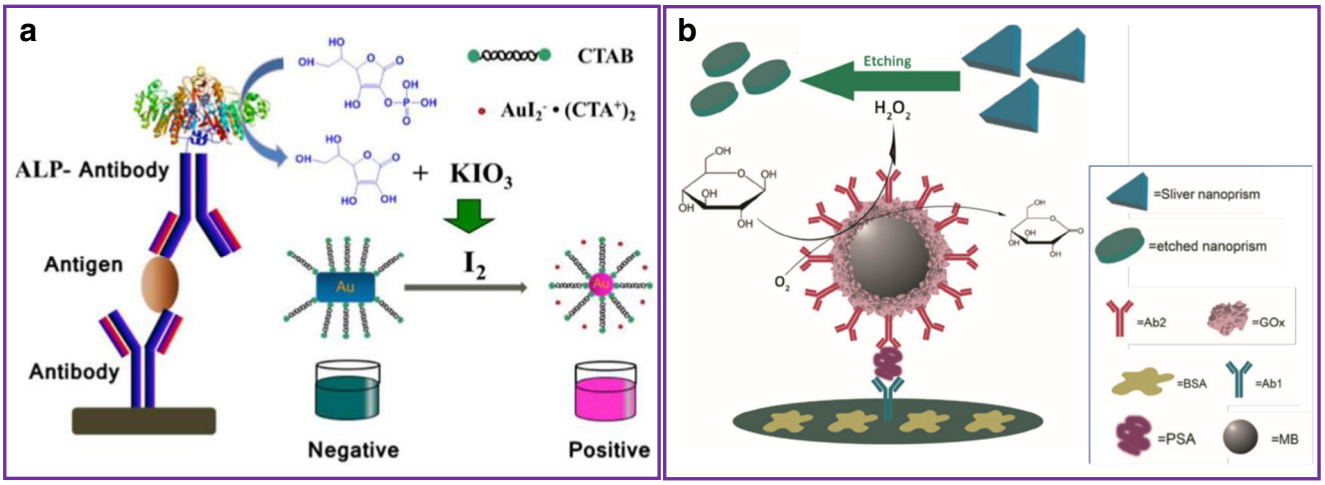

Fig. 7 Schematic diagram of AuNRs and AgNPRs etching in P-ELISA. **a** Schematic diagram of ALP-triggered etching of AuNRs. Reproduced with permission from Ref. [55]. Copyright American Chemical Society, 2015. **b** Schematic diagram of GOx-triggered etching of AgNPRs. Reproduced with permission from Ref. [78]. Copyright Elsevier, 2015

Noble metal NPs by adjust the formation of AuNPs to change the colour and DLS of the solution

Based on reduction $HAuCl_4$ to form AuNPs, Huang's group fabricated an ethylene diamine tetraacetic acid (EDTA)-triggered assay for detection of disease biomarker and drug [81]. In the assay, the analyte-recognizable antibody was labeled with EDTA which catalyzed decomposition of H_2O_2 and adjusted the growth of H_2O_2-induced formation of AuNPs with color variation. Through combining with a sandwich immunoassay, a various color AuNPs suspension can be obtained as a read-out means (Fig. 9). The fabricated sensitive assay allows for naked-eye detection of cancer antigen15-3 and small molecular drug methamphetamine with high accuracy.

In the growth based immunoassay, the factors including ageing of the solutions, type of reaction vessel and reaction scale of the system can interfere and result in false positive results. The etching based immunoassay is the mainly robust to the field conditions compared to other approaches such as aggregations, growth and metallization of NPs.

Noble metal NPs serving as catalysts (enzyme mimics)

Noble metal NPs itself as catalysts (enzyme mimics) to catalyze substrates to trigger a detectable signal

Wei and Wang reviewed various NPs with enzyme-like characteristics mainly focused on their kinetics, mechanisms, the activity tuning of catalysts, as well as applications in numerous fields [82]. Metal NPs not only can enhance the activities of HRP [83], but also have unique peroxidase-like activity which can catalytic oxidation of peroxidase substrate 3,3,5,5-tetramethylbenzidine (TMB) with H_2O_2 [84]. These

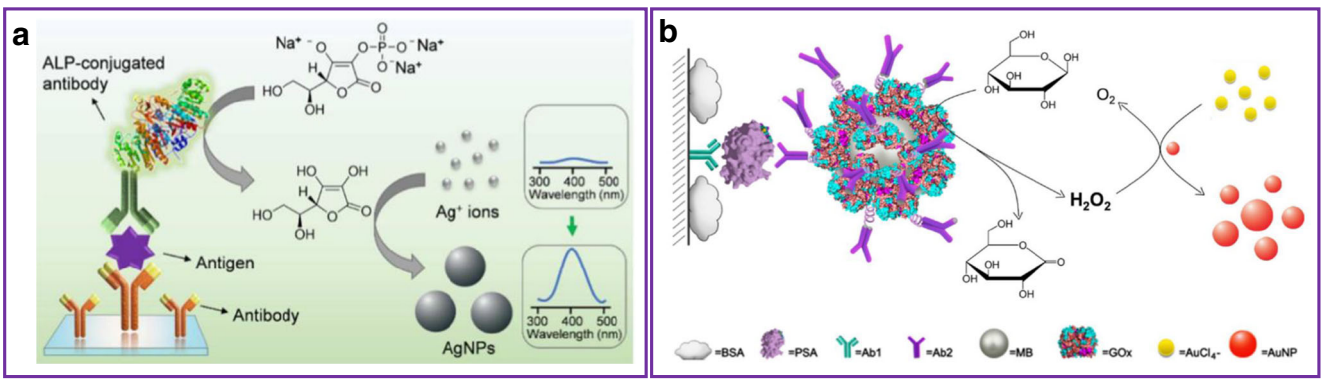

Fig. 8 Schematic diagram of AgNPs and AuNPs growth in immunoassay. **a** Schematic diagram of ALP-mediated growth of AgNPs. Reproduced with permission from Ref. [79]. Copyright Royal Society of Chemistry, 2016. **b** Schematic diagram of GOx-catalyzed growth of AuNPs. Reproduced with permission from Ref. [80]. Copyright American Chemical Society, 2014

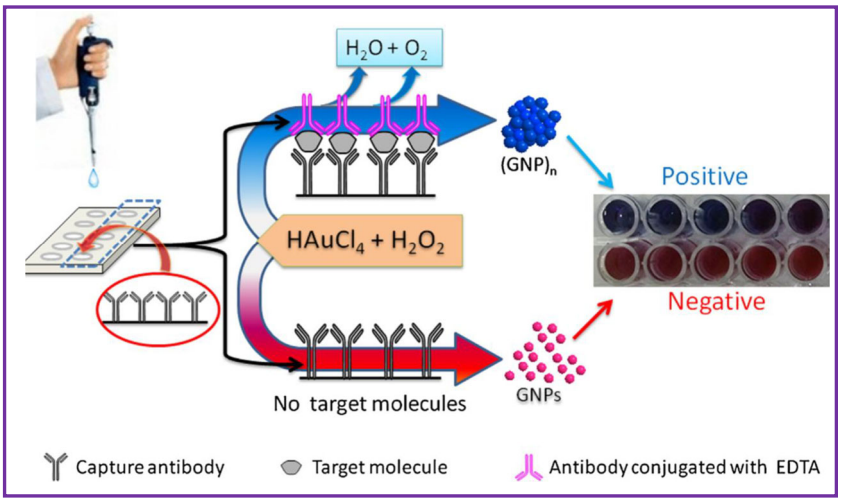

Fig. 9 Schematic diagram of ELISA-like assay based on EDTA-triggered AuNPs formation. Reproduced with permission from Ref. [81]. Copyright Elsevier, 2017

findings open up a wide range of new potential applications of metal NPs in immunoassays.

Metal NPs, such as Pt, Au and Ag NPs have more active sites on their surface than enzymes, usually just only one site. Thus, when they are used as enzyme mimics, signals are generated at many active sites per NP allowing higher signal amplification [85–89]. Gao and coworkers first reported the intrinsic peroxidase-like activity of Fe_3O_4 NPs which catalysed the reaction of peroxidase substrates to give the same colour changes as HRP. The catalysis showed typical Michaelis-Menten kinetics and H_2O_2, pH and temperature dependence. Based on this finding, they proposed a novel immunoassay by using Fe_3O_4 NPs as functions of capture, separation and detection tools [90]. Duan and coworkers developed a nanozyme-strip for the detection of Ebola virus by using Fe_3O_4 NPs as a nanozyme probe [91]. The diagnostic accuracy for clinical samples is comparable with ELISA, while the performance of the nanozyme-strip is much faster (within 30 min) and simpler (without need of any equipments and specialist). The sensitivity (1 ng/ml) is 100-fold more sensitive than that of traditional lateral flow assay (100 ng/ml). Syed Rahin Ahmed and coworkers also designed a modified ELISA for the detection of Influenza Virus by using the peroxidase-mimic of AuNPs for signal amplification (Fig. 10). The sensitivity improves to 500-fold higher than that of commercial virus kits [87].

Noble metal NPs doped or combining with other nanomaterials as catalysts to catalyze substrates to trigger a detectable signal

Natural enzymes have critical limitations for immunoassay application, such as low stability under harsh temperature and pH conditions. To overcome these limitations, various nanostructures have been synthesized as enzyme mimics for signal amplification of immunoassay. Nanohybrids with nanostructures exhibit amazing synergistic effects to enhance the catalytic activity that can be used in the field of biosensors and immunoassays. The combing nanostructures of metal NPs with other material as artificial enzymes have been intensively studied for colorimetric and electrochemical immunoassays [4, 86, 92–95].

For example, Wang and coworkers fabricated a powerful enzyme mimic by loading Pt nanocatalysts on hydrophobic carbon nanotubes (CNTs) which were dispersed in graphene

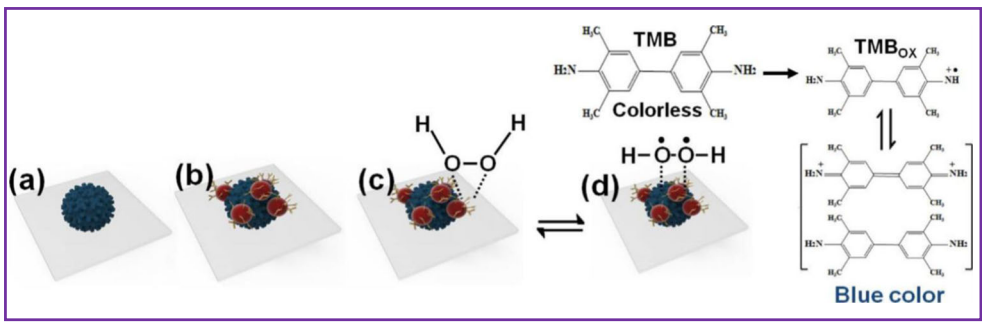

Fig. 10 Schematic diagram of peroxidase-mimic enzymatic reaction of AuNPs. **a** viruses coated on a polystyrene 96-well plate, **b** antibody-AuNPs conjugate bound with virus through immunoreactions, **c** TMB-H_2O_2 added and **d** color changes due to peroxidase-mimic activity of AuNPs. Reproduced with permission from Ref. [87]. Copyright WILEY-VCH, 2016

oxide (GO) nanocolloids. The nanohybrids exhibits greatly enhanced peroxidase-like catalysis comparable to natural enzymes. An electrochemical immunoassay has been successfully developed using the nanohybrids GO-CNT–Pt as catalysts [94]. Park's group synthetized a hybrid structure of graphene-AuNPs and designed a colorimetric immunoassay by using antibody conjugated graphene-AuNPs for sensitive detection of norovirus-like particles in human serum (Fig. 11**a**). The sensitivity (92.7 pg/mL) is 112 times higher than that of a conventional ELISA (10.4 ng/mL) [92]. Park's group also produced nanohybrids composed of AuNPs and CNTs. The AuNP-CNT nanohybrids shows enhanced peroxidase-like catalytic activity which is used as part of an ultrasensitive colorimetric test for influenza virus A (Fig. 11**b**). The detection limit (3.4 PFU/ml) shows 385 times lower than that of conventional ELISA (1312 PFU/ml) [93].

Based on N-doped graphene nanoribbons immobilized Fe-based-Metal-organic frameworks deposited with AuNPs (N-GNRs-Fe-MOFs@AuNPs) nanocomposites, Tang and coworkers designed a sensitive sandwich-type electrochemical immunoassay for the detection of galectin-3 (Gal-3) [15]. A glassy carbon electrode (GCE) was modified with AuNPs immobilized by Ab_1 against Gal-3. Methylene blue (MB) as an electron transfer mediators was responsible for electron production and signal amplification. The Ab_2 against Gal-3 was combined with AuPt-MB nanohybrids which displayed redox-active, uniform morphology and good electrochemical activity to generate and amplify the electrochemical signal. The sandwich type format of N-GNRs-Fe-MOFs@AuNPs-Ab_1 coupled with AuPt-MB-Ab_2 greatly enhanced the immunoassay's sensitivity (Fig. 12**)**.

Fe_3O_4 NPs coupling with other nanomaterials, can accelerate catalytic activity in various signal amplification strategies in electrochemical immunoassays [1, 96–98]. For example, Wei and coworkers fabricated an ultrasensitive photoelectrochemical (PEC) immunoassay for the detection of microcystin-LR (MC-LR) based on Fe_3O_4 NPs/polydopamine (Fe_3O_4@PDA) which was used as the label carrier to conjugate the Ab_2 and HRP. CdS/TiO_2 nanorod arrays, having high photo-to-current conversion efficiency were used as a sensitive PEC material to immobilize antigens. After the specific immunoreaction of MC-LR with its antibody, the photocurrent change was amplified due to the synergistically accelerate catalytic activity of Fe_3O_4 NPs and HRP on the electrode surface [1]. Wu and coworkers designed an ultrasensitive electrochemical immunoassay by using the synergetic effect of dumbbell-like Pt-Fe_3O_4 NPs in catalyzing H_2O_2 reduction for squamous cell carcinoma antigen (SCC-Ag) [98]. The Ab_1 specific for SCC was immobilized onto nitrogen-doped graphene sheets modified glassy carbon electrode. The Pt-Fe_3O_4 NPs were used as carrier for loading the Ab_2 (Fig. 13**a**). The synergetic effect of Pt-Fe_3O_4 NPs results in the high sensitivity of the assay. Liu's group also developed a highly sensitive electrochemical immunoassay for detection of chlorpyrifos. The glass carbon electrode was modified with polydopamine nanospheres (PDANSs) as the assay platform. Fe_3O_4 NPs was coated on CNTs as the signal label. The flake-like CNTs@f-Fe_3O_4 nanocomposites possessing large surface area was used as carrier for loading abundant of Ab_2 and HRP (Fig. 13**b**). The high sensitivity of the assay is achieved attributed to the peroxidase-mimic activity of Fe_3O_4 [96].

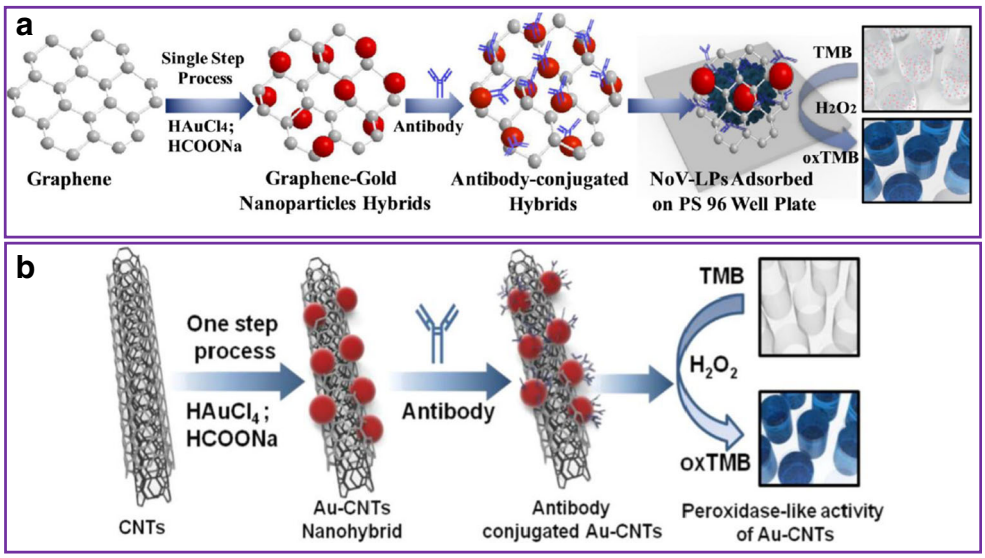

Fig. 11 Schematic diagram of AuNPs combining with other nanomaterials as catalysts. **a** Schematic illustration of graphane-AuNPs nanohybrids as enhanced peroxidase-like catalysis in colorimetric immunoassay. Reproduced with permission from Ref. [92]. Copyright Elsevier, 2017. **b** Schematic illustration of CNTs-AuNPs nanohybrids as enhanced peroxidase-like catalysis in colorimetric test. Reproduced with permission from Ref. [93]. Copyright Elsevier, 2016

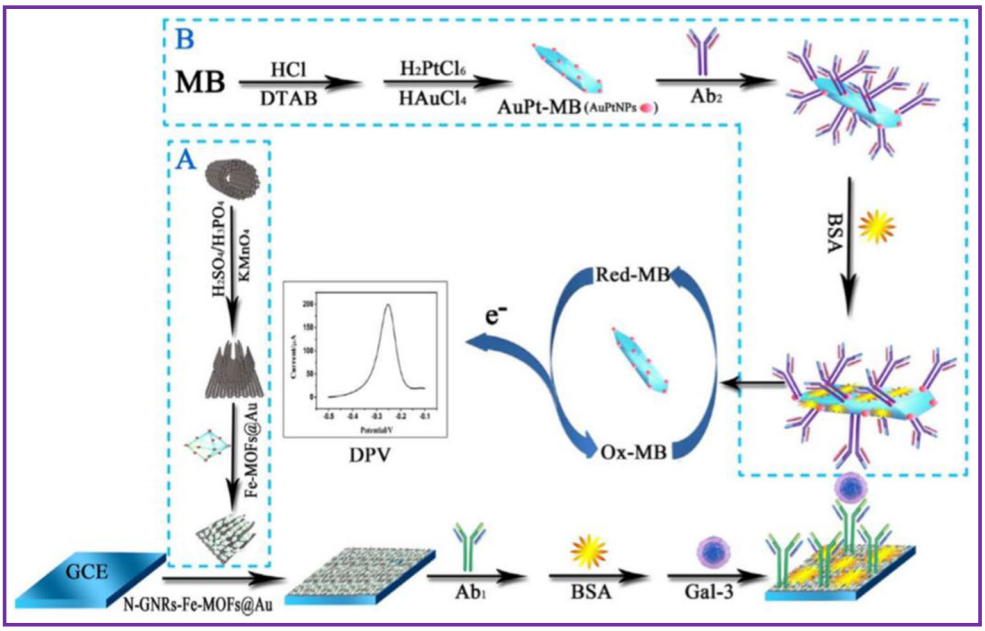

Fig. 12 Schematic diagram of doped metal NPs nanocomposites as catalysts in sandwich-type electrochemical immunoassay. Reproduced with permission from Ref. [15]. Copyright Elsevier, 2017. **a** Schematic illustration of N-GNRs-Fe-MOFs@AuNPs. **b** Schematic illustration of AuPt-MB-Ab_2

The enzyme activity of metal NPs is mainly dependent on particle size. After loading more biomoleculars, the enzyme activity of metal NPs decrease even disappear. These limit the usage of metal NPs as enzyme mimics in immunoassays. Table 5 sumarizes the metal NPs used as catalysts.

Noble metal NPs serving as in synergistic effects

Metal NPs have synergistic effect for biocompatibility and conductivity to enhance signal transduction producing amplify

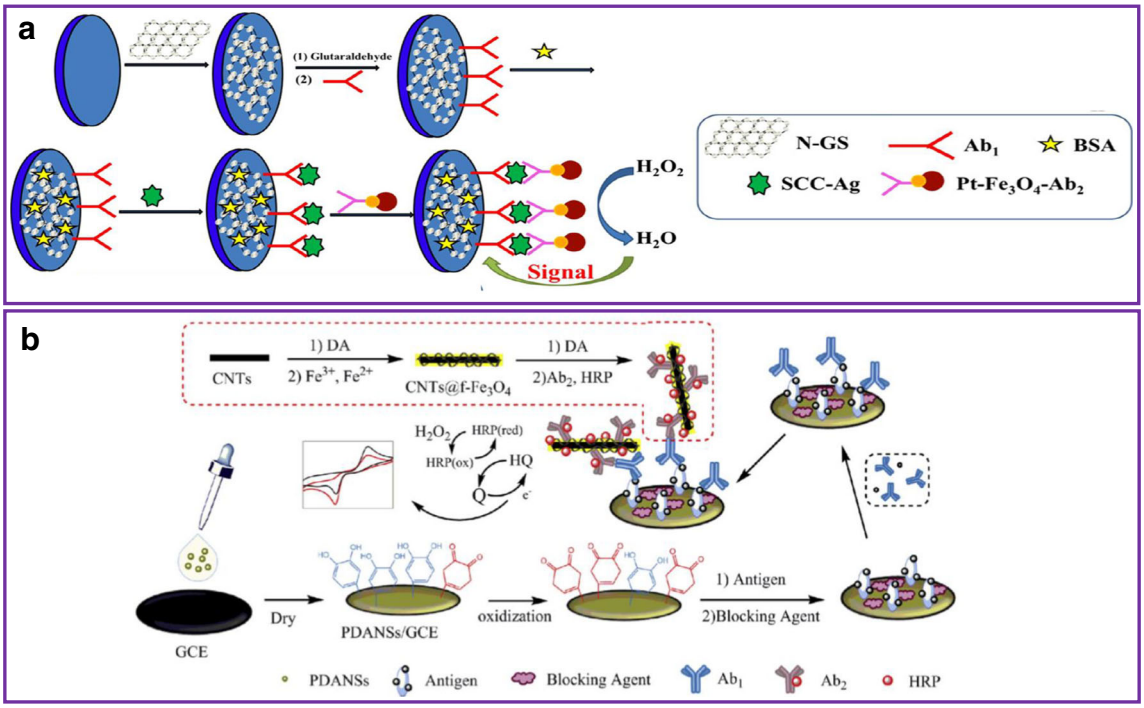

Fig. 13 Schematic diagram of catalytic activity of Fe_3O_4 NPs combining with other nanomaterials as catalysts in electrochemical immunoassay. **a** Schematic illustration of dumbbell-like Pt-Fe_3O_4 NPs in catalyzing H_2O_2 reduction. Reproduced with permission from Ref. [98]. Copyright Elsevier, 2013. **b** Schematic illustration of flake-like CNTs@f-Fe_3O_4 nanocomposites as peroxidase-mimic activity. Reproduced with permission from Ref. [96]. Copyright Elsevier, 2015

Table 5 An overview on metal NPs used as catalysts in immunoassays

Particle type	Principle	Targets	Limit of detection	Measurement range	Reference
AuNPs [1]	ELISA	Influenza virus	10 PFU/mL	N [2]	[99]
AuNPs	Colorimetric assay	H_2O_2; Glucose.	5×10^{-7} M; 4×10^{-6} M	2.0×10^{-6}-2.0×10^{-4} M; 1.8×10^{-5}-1.1×10^{-3} M	[84]
AuNPs@CNT	Surface-enhanced Raman scattering	Influenza virus	3.4 PFU/mL	10-50,000 PFU/mL	[93]
Graphene@AuNPs	Spectroscopic analysis	Norovirus-like particles	92.7 pg/ mL	100 pg/ mL-10 μg/mL	[92]
Ag@AuNPs	Electrochemical measurement	Human IgG	23 fg/mL	5.0×10^{-8}-7.5×10^{-7} μg/mL	[88]
Fe_3O_4	Strip	Ebola	1 ng/mL	N [a]	[91]
Fe3O4/PANI@Nafion	Electrochemical immunosensor	Benzo[a]pyrene	4 pM	8 pM-2 nM	[97]
CNTs@f-Fe_3O_4	Electrochemical immunoassay	Chlorpyrifos	6.3 pg/mL	0.1-1000 ng/ mL	[96]
PtNPs	Photoelectrochemical immunoassay	Mouse IgG	6.0 fg/mL	0.01 pg/mL-1.0 ng/mL	[95]
Fe_3O_4@Pt	Electrochemical immunosensor	Cancer biomarker squamous cell carcinoma antigen	15.3 pg/mL	0.05-18 ng/mL	[98]

[1] Nanoparticles; [2] Not provided;

recognition events with designed signal tags. Association of different metal NPs or metal NPs with other nanocomposits can escalate the signal amplification effect [100, 101]. For instance, utilizing the superior photoelectric properties of Zinc Oxide (ZnO) and the better electron transportation property of AuNP, the amalgamating ZnO with AuNP can result in more sensitive response against SK-BR-3 cancer cells [102] and Carcinoembryonic antibody [103]. Several metal NPs have been simultaneously employed in one or multiple signal amplification strategies in an immunoassay [6, 13, 104–129] (Table 6).

Using ZnO-label/cadmium sulfide (CdS)-staining and enhanced cathodic preconcentration/in-situ anodic stripping voltammetry (ASV) analysis of the stained CdS, Qin and coworkers fabricated an ultrasensitive metal-labeled amperometric immunoassay for human IgG and human heart-type fatty-acid-binding protein. In the assay, the glassy carbon electrode (GCE) was modified with β-cyclodextrin-graphene sheets (CD-GS) nanocomposite. BSA, Ab_1, antigen and ZnO-multiwalled carbon nanotubes (MWCNTs) labeled Ab_2 (Ab_2-ZnO-MWCNTs) were anchored on the CD-GS nanocomposite through an immunoreaction, forming a sandwich-type immunoelectrode (Ab_2-ZnO-MWCNTs/antigen/BSA/Ab_1/CD-GS/GCE). The following in-situ ASV detection was used for sensitive enhanced immunoassay [6]. Feng and coworkers fabricated a PEC immunoassay based on TiO_2/S-$BiVO_4$@Ag_2S composites by layer-by-layer method for quantitative detection of the ochratoxin A (OTA). TiO_2 has good photoelectric activity and large surface area. The S-$BiVO_4$ has porous structure surfaces which is beneficial for the sufficient in-situ growth of Ag_2S NPs with high absorb visible-light. The cascade band-edge levels of assembled TiO_2/S-$BiVO_4$@Ag_2S composites promote ultrafast transfer of charge and effectively inhibited the recombination of e^-/h^+ pairs. Consequently, the response of photocurrent was enhanced and the conversion efficiency of photocurrent was improved [13]. Based on Graphene/chitosan-ferrocene (GO/CS-Fc) and Fe_3O_4/AuNPs as the assay platform, Peng and coworkers designed a novel electrochemical immunoassay for the detection of carcinoembryonic antigen (CEA). Due to possessing high surface area, GO/CS-Fc was used as carrier for loading a large amount of Ab_1. Fe_3O_4/AuNPs were labeled with Ab_2. After the immunoreactions, a sandwich structure GO/CS-Fc/Ab_1-CEA-Ab_2/Fe_3O_4/AuNPs was formed. The redox cycling efficiency was enhanced by introducing the Fe_3O_4/AuNPs/Ab_2 onto the electrode surface (Fig. 14). Based on the redox cycling amplification strategy, the detection signal (30 μA) is 10-fold increased compared to that without Fe_3O_4/Au NPs labeling (3 μA) [130].

Using gold-silver hollow microspheres (AuAgHSs) as labels, Tang and coworkers fabricated a dual signal amplification strategy in electrochemical immunoassay for the detection of carcinoembryonic antigen (CEA used as model analyte) [106]. The amplification of the electrochemical signal

Table 6 An overview on metal NPs serving as in synergistic effects in immunoassays

Particle type	Principle of signal output	Targets	Limit of detection	Measurement range	Reference
AuNPs [1]/(CdS, PbS and Au)	Bidirectional stripping voltammetric immunoassay	Cancer biomarkers (AFP, CEA and CA19-9)	0.02, 0.05 and 0.3 pg/mL	1 pg/mL-50 ng/mL, 1 pg/mL-50 ng/mL, 5 pg/mL-100 ng/mL	[133]
Fe_3O_4/AuNPs	Electrochemical immunosensor	Carcinoembryonic antigen	0.39 pg/mL.	0.001-30 ng/mL	[134]
TiO_2/CdS/CdSe	Photoelectrochemical immunoassay	Interleukin-6	0.38 pg/mL	1.0 pg/mL- 100 ng/mL	[135]
SiO_2@PAA@CAT	Plasmonic ELISA	Ochratoxin A	5×10^{-20} g/mL	10^{-12}-10^{-20} g/mL	[136]
Ferrocenemonocarboxylic–HRP@PtNPs	Electro-immunosensing	γ-fetoprotein	1.7 pg/mL.	0.005-20 ng/mL	[137]
PdAu/ZnO@CdTe QDs	Photoelectrochemical immunoassay	Carcinoembryonic antigen	0.33 pg/mL	0.001-90 ng/mL	[138]
Carbon nanospheres@ AuNPs (AgNPs)	Multiplexed electrochemical immunosensor	Carcinoembryonic antigen and γ-fetoprotein	2.8 and 3.5 pg/mL	0.01-80 ng/mL	[139]
Polydopamine @AgNPs/polydopamine@AuNPs /CQDs-PEI-GO	Electrochemiluminescence immunosensor	Carcinoembryonic antigen	1.67 pg/mL	5 pg/mL-500 ng/mL	[77]
ZnO@CNT/Pt/Au alloy	Electrochemiluminescence detection	Prostate specific antigen	0.61 pg/mL	0.001-500 ng/mL	[80]
ZnO@graphene	Photoelectrochemical detection	Cancer cells	58 cells/mL	10^2-10^6 cells/mL	[140]
Fe_3O_4@Ag/Au@Ag NRs [2]	Surface-enhanced resonance Raman scattering sensor	cancer biomarkers.	4.75 fg/mL	10 fg/mL-100 ng/mL	[141]
Fe_3O_4/CdTe@CDs	Electrochemiluminescence	Squamous cell carcinoma antigen	6.3 fg/mL	0.02-12 ng/mL	[142]
AuAg hollow microspheres@ Prussian blue NPs	Electrochemical immunosensor	Carcinoembryonic antigen	1.0 pg/mL	0.005-50 ng/mL	[143]
Graphene@PtNPs	Electrochemical immunoassay	Carcinoembryonic antigen; α-fetoprotein	1.64-1.33 pg/mL	0.01-100 ng/mL	[144]
CdS@Cu_2O/porous ZnO@carbon nanotubes	Photoelectrochemical immunoassay	Carcinoembryonic antigen	0.4 pg/mL	1.0 pg/mL-80 ng/mL	[118]
GMCs@AuNP/ polyamidoamine@Au electrode	Electron immunosensor	Penicillin binding protein	0.65 pg/mL	0.025-6.4 ng/mL	[145]
AuNPs/Fe_3O_4	ELISA	Respiratory syncytial virus	0.021 pg/mL	0.1-30 pg/mL	[146]
AgNPs-AuNPs@polypyrrole microsphere	Electrochemical immunosensor	Microcystin-LR	0.1 ng/mL	0.25 ng/mL-50 μg/mL	[114]
AuNPs/SiO_2@ PAA	Plasmonic ELISA	Tetrabromobisphenol A derivative and byproduct	3.3×10^{-4} ng/mL	10^{-3}-10^3 ng/mL	[147]

[1] Nanoparticles; [2] Nanoprism

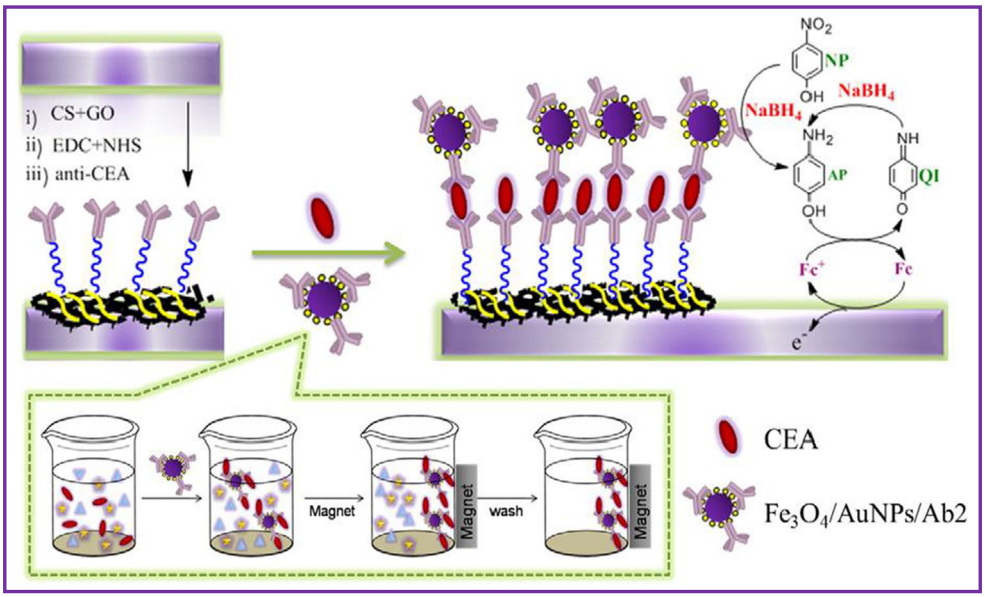

Fig. 14 Schematic diagram of GO/CS-Fc and Fe_3O_4/AuNPs based electrochemical immunosensor. Reproduced with permission from Ref. [130]. Copyright Elsevier, 2015

was based on the catalytic recycling of the product with the aid of the labeled GOx on the AuAgHSs and the immobilized prussian blue nanoparticles (PBNPs) on the graphene nanosheets. With a sandwich-type immunoassay on the graphene-based platform, the first signal amplification was introduced based on the catalytic oxidation of glucose by GOx labeled on the AuAgHSs. The generated H_2O_2 was catalytically reduced by PBNPs immobilized on the electrode with the second amplification. Lin and coworkers also designed a dual signal amplification strategy based electrochemical immunoassay for ultrasensitive detection of benzo[a]pyrene (BaP). Fe_3O_4/polyaniline/Nafion (Fe_3O_4/PANI) nanocomposites were assembled on the surface of Nafion/ITO as assay platform to capture BaP. Fe_3O_4 NPs in the Fe_3O_4/PANI nanocomposites served as a mimetic peroxidase to catalyze the reduction of H_2O_2, providing a good pathway of electron transfer. Highly-carbonized spheres (HCS) were used as nanocarrier for loading HPR and Ab_2. After competitive immunoreactions between the BaP on the assay platform and BaP in the sample solution with the Ab_1, multi-HRP-HCS-Ab_2 label was capture by Ab_1 on the assay platform (Fig. 15**a**). The enhanced signal of catalytic current was achieved by using Fe_3O_4/PANI nanocomposites as the multiplex binding biomimetic peroxidase for the reduction of H_2O_2 [97].

Combing the high loading capacity of MBs for ALP and ALP-triggered dispersion of aggregated AuNPs, Zhan and coworkers proposed a dual-signal amplified P-ELISA for sensitive detection of respiratory syncytial virus [113]. In this assay, MBs were employed as carrier to load large amount of ALP molecules for signal amplification. The introduction of Zn^{2+} to the detection system induced the accelerated dephosphorylation reaction of ALP to trigger the dispersion of aggregated AuNPs, resulting in the amplification of the signal (Fig. 15**b**). The sensitivity of the P-ELISA (0.021 pg/mL) exceed that of conventional ELISA (1 pg/mL) by about 50 times.

Based on both AuNPs and electro-active indicator labeled rolling circle amplification, Su and coworkers developed a multiple signal amplification electrochemical immunoassay

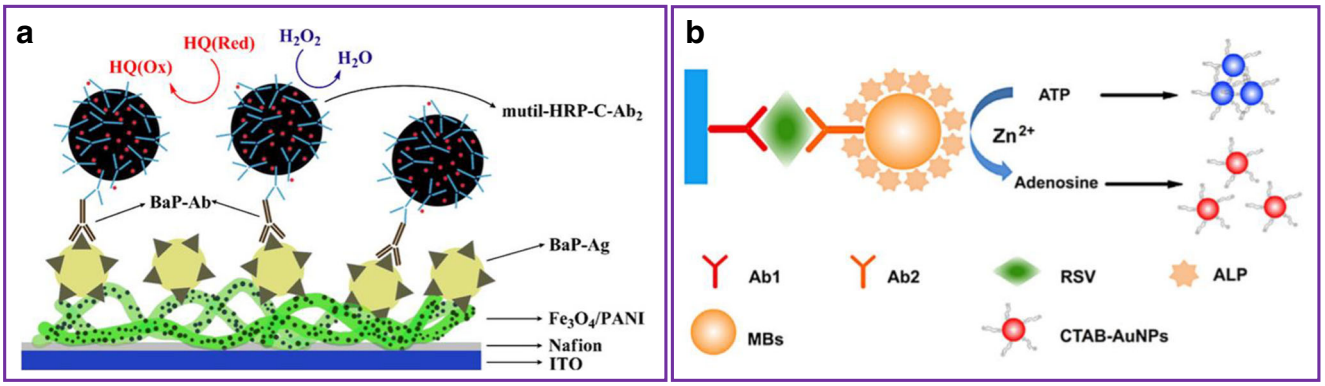

Fig. 15 Schematic diagram of different metal NPs in signal dual-amplification strategy. **a** Schematic illustration of Fe_3O_4/PANI nanocomposites based electrochemical immunoassay. Reproduced with permission from Ref. [97]. Copyright Elsevier, 2012. **b** Schematic illustration of MBs-ALP-triggered AuNPs aggregation in P-ELISA. Reproduced with permission from Ref. [113]. Copyright Elsevier, 2017

for the detection of alpha-fetoprotein. In the assay, AuNPs were used as carrier for loading a large amount of primary DNA, Pt NPs were used as the carrier of ferrocenemonocarboxylic (Fc) and HRP. After an immuno-sandwich protocol, the conjugates of primary DNA and Ab_2 acted as a precursor to initiate rolling circle amplification. The enzymatic signals were amplified by the catalysis of HRP and Pt NPs with the addition of H_2O_2. The multiple amplified signals lead to low detection limit of alpha-fetoprotein [105]. Based on enzyme-mediated AuNP growth and silica NPs carrying poly acrylic acid nanospherical brushes (SiO_2@PAA@CAT/GOx), multiple signal amplification strategy P-ELISAs have been developed [127, 131, 132]. For example, based on CAT-mediated AuNP growth and silica NPs carrying poly acrylic acid nanospherical brushes (SiO_2@PAA@CAT), Huang and coworkers designed a P-ELISA for ultrasensitive detection of disease-related biomarker ochratoxin A (OTA) by using sandwich formats [131]. SiO_2@PAA was not only served as a "CAT container" (SiO_2@PAA@CAT) to generate a signal amplification, but also used as a regulator to adjust the binding ability between competitive antigens and antibodies because of its relatively greater volume weight (Fig. 16). The LODs of the proposed P-ELISA are at least 7 orders lower than that of competitive CAT-based P-ELISA (by the naked eye) and 8 orders lower than that of HRP-based conventional ELISA (by the microplate reader), respectively. Based on the same principle, Zhang and coworkers proposed another P-ELISA using SiO_2@PAA@GOx nanospherical brushes for detection of Typical Tetrabromobisphenol A Derivative and Byproduct [132]. The sensitivity of the method (3.3×10^{-4} μg/L) is 3 orders of magnitude higher than that using conventional colorimetric ELISA with the same antibody (0.7018 μg/L).

Although the synergistic effects of metal NPs can escalate the signal amplification of the assay. Association of more metal NPs or other nanocomposits makes the system of the assay more complicated.

Conclusions and perspectives

Considerable progresses of noble metal NPs based signal amplification strategies in immunoassays have been made in recent years. However, the following significant issues are still deserved in-depth exploration. (1) Integration of different

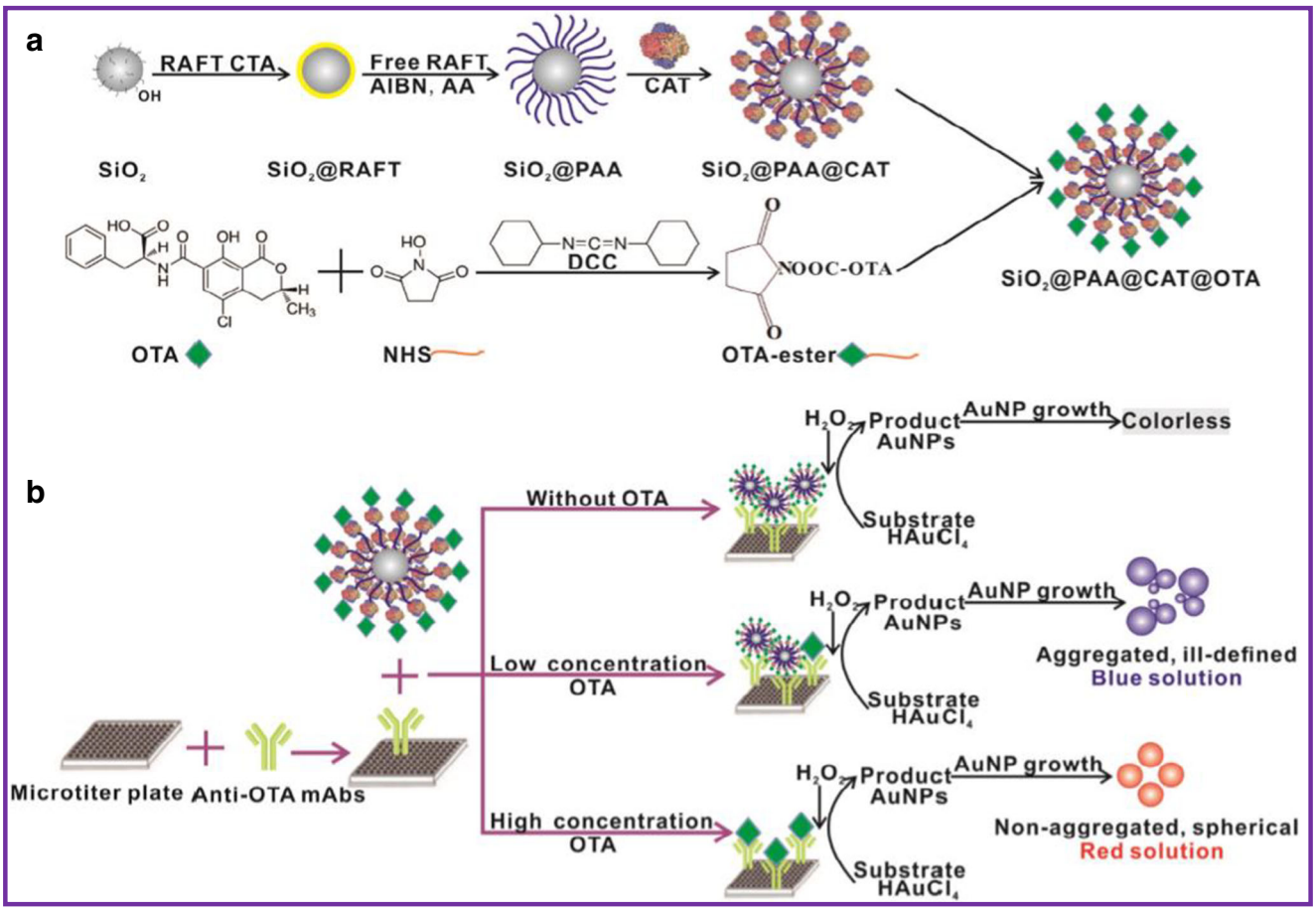

Fig. 16 Schematic diagram of SiO_2@PAA@CAT@OTA based P-ELISA. Reproduced with permission from Ref. [131]. Copyright American Chemical Society, 2016. **a** Schematic illustration of SiO_2@PAA@CAT@OTA preparation, **b** Schematic diagram of P-ELISA based on CAT-catalyzed growth of AuNPs

techniques. The integration of metal NPs based signal amplification strategies with other techniques, such as nanofluidics, electrochemistry, molecular biology, biophysics and multiplexing methodologies provide possibilities for fabrication of new ultrasensitive immunoassay. (2) Combining of multiple signal amplification strategies. The combination of different signal amplification strategies in one immunoassay is an avenue for development of new ultrasensitive immunoassay. (3) Generation of new nanohybrids. To generate new nanohybrids with enhanced catalytic activity, higher stability and lower toxicity for signal amplification strategy applications is also highly desirable. (4) Synergy research for noble metal NPs each other or with other nanomaterials. The synergy research both in experiments and theories is needed for fundamental understanding and better applications of noble metal NPs in signal amplification strategy. Using synergies of noble metal NPs each other or with other nanomaterials should be tailored for the design of novel signal amplification strategy.

Acknowledgements The authors are thankful to the financial support of the National Key R&D Program of China (grant numbers 2018YFC1602500, 2017YFC1601205) and the National Natural Science Foundation of China (grant numbers 31601536, 31871888).

Compliance with ethical standards

Competing interests The authors declare that they have no competing interests.

References

1. Wei J, Qileng A, Yan Y, Lei H, Zhang S, Liu W, Liu Y (2017) A novel visible-light driven photoelectrochemical immunosensor based on multi-amplification strategy for ultrasensitive detection of microcystin-LR. Anal Chim Acta 994:82–91
2. Sun Q, Luo J, Zhang L, Zhang Z, Le T (2018) Development of monoclonal antibody-based ultrasensitive enzyme-linked immunosorbent assay and fluorescence-linked immunosorbent assay for 1-aminohydantoin detection in aquatic animals. J Pharm Biomed Anal 147:417–424
3. Li L, Niu C, Li T, Wan Y, Zhou Y, Wang H, Yuan R, Liao P (2018) Ultrasensitive electrochemiluminescence biosensor for detection of laminin based on DNA dendrimer-carried luminophore and DNA nanomachine-mediated target recycling amplification. Biosens Bioelectron 101:206–212
4. Jiang W, Wu L, Duan J, Yin H, Ai S (2018) Ultrasensitive electrochemiluminescence immunosensor for 5-hydroxymethylcytosine detection based on Fe3O4@SiO2 nanoparticles and PAMAM dendrimers. Biosens Bioelectron 99:660–666
5. Wang X, Gao P, Yan T, Li R, Xu R, Zhang Y, Du B, Wei Q (2018) Ultrasensitive photoelectrochemical immunosensor for insulin detection based on dual inhibition effect of CuS-SiO 2 composite on CdS sensitized C-TiO 2. Sensors Actuators B Chem 258:1–9
6. Qin X, Xu A, Liu L, Sui Y, Li Y, Tan Y, Chen C, Xie Q (2017) Selective staining of CdS on ZnO biolabel for ultrasensitive sandwich-type amperometric immunoassay of human heart-type fatty-acid-binding protein and immunoglobulin G. Biosens Bioelectron 91:321–327
7. Jalal UM, Jin GJ, Eom KS, Kim MH, Shim JS (2018) On-chip signal amplification of magnetic bead-based immunoassay by aviating magnetic bead chains. Bioelectrochemistry 122:221–226
8. Cui L, Li Y, Lu M, Tang B, Zhang CY (2018) An ultrasensitive electrochemical biosensor for polynucleotide kinase assay based on gold nanoparticle-mediated lambda exonuclease cleavage-induced signal amplification. Biosens Bioelectron 99:1–7
9. Liu L, Chang Y, Xia N, Peng P, Zhang L, Jiang M, Zhang J, Liu L (2017) Simple, sensitive and label-free electrochemical detection of microRNAs based on the in situ formation of silver nanoparticles aggregates for signal amplification. Biosens Bioelectron 94: 235–242
10. Zhou J, Tang J, Chen G, Tang D (2014) Layer-by-layer multienzyme assembly for highly sensitive electrochemical immunoassay based on tyramine signal amplification strategy. Biosens Bioelectron 54:323–328
11. Zhang Y, Sun G, Yang H, Yu J, Yan M, Song X (2016) Multifunctional reduced graphene oxide trigged chemiluminescence resonance energy transfer: Novel signal amplification strategy for photoelectrochemical immunoassay of squamous cell carcinoma antigen. Biosens Bioelectron 79:55–62
12. Wang HY, Qi CL, He WH, Wang MH, Jiang WJ, Yin HS, Ai SY (2018) A sensitive photoelectrochemical immunoassay of N^6-methyladenosine based on dual-signal amplification strategy: Ru doped in SiO_2 nanosphere and carboxylated g-C_3N_4. Biosens Bioelectron 99:281–288
13. Feng J, Li Y, Gao Z, Lv H, Zhang X, Fan D, Wei Q (2018) Visible-light driven label-free photoelectrochemical immunosensor based on TiO2/S-BiVO4@Ag2S nanocomposites for sensitive detection OTA. Biosens Bioelectron 99:14–20
14. Zhang X, Guo W, Wang Z, Ke H, Zhao W, Zhang A, Huang C, Jia N (2017) A sandwich electrochemiluminescence immunosensor for highly sensitive detection of alpha fetal protein based on MoS 2 -PEI-Au nanocomposites and Au@BSA core/shell nanoparticles. Sensors Actuators B Chem 253:470–477
15. Tang Z, He J, Chen J, Niu Y, Zhao Y, Zhang Y, Yu C (2018) A sensitive sandwich-type immunosensor for the detection of galectin-3 based on N-GNRs-Fe-MOFs@AuNPs nanocomposites and a novel AuPt-methylene blue nanorod. Biosens Bioelectron 101:253–259
16. Zeng S, Yong K-T, Roy I, Dinh X-Q, Yu X, Luan F (2011) A Review on Functionalized Gold Nanoparticles for Biosensing Applications. Plasmonics 6:491–506
17. Doria G, Conde J, Veigas B, Giestas L, Almeida C, Assuncao M, Rosa J, Baptista PV (2012) Noble metal nanoparticles for biosensing applications. Sensors 12:1657–1687
18. Xia Y (2016) Optical sensing and biosensing based on nonspherical noble metal nanoparticles. Anal Bioanal Chem 408: 2813–2825
19. Willets KA, Van Duyne RP (2007) Localized surface plasmon resonance spectroscopy and sensing. Annu Rev Phys Chem 58:267–297
20. Saha K, Agasti SS, Kim C, Li X, Rotello VM (2012) Gold nanoparticles in chemical and biological sensing. Chem Rev 112: 2739–2779
21. Vilela D, Gonzalez MC, Escarpa A (2012) Sensing colorimetric approaches based on gold and silver nanoparticles aggregation: chemical creativity behind the assay. A review. Anal Chim Acta 751:24–43
22. Rycenga M, Cobley CM, Zeng J, Li W, Moran CH, Zhang Q, Qin D, Xia Y (2011) Controlling the synthesis and assembly of silver nanostructures for plasmonic applications. Chem Rev 111:3669–3712

23. Baryeh K, Takalkar S, Lund M, Liu G (2017) Development of quantitative immunochromatographic assay for rapid and sensitive detection of carbohydrate antigen 19-9 (CA 19-9) in human plasma. J Pharm Biomed Anal 146:285–291
24. Xiao M, Fu Q, Shen H, Chen Y, Xiao W, Yan D, Tang X, Zhong Z, Tang Y (2018) A turn-on competitive immunochromatographic strips integrated with quantum dots and gold nano-stars for cadmium ion detection. Talanta 178:644–649
25. Wen-de W, Min L, Ming C, Li-Ping L, Rui W, Hai-Lan C, Fu-Yan C, Qiang M, Wan-Wen L, Han-Zhong C (2017) Development of a colloidal gold immunochromatographic strip for rapid detection of Streptococcus agalactiae in tilapia. Biosens Bioelectron 91:66–69
26. Lee D, Kim YT, Lee JW, Kim DH, Seo TS (2016) An integrated direct loop-mediated isothermal amplification microdevice incorporated with an immunochromatographic strip for bacteria detection in human whole blood and milk without a sample preparation step. Biosens Bioelectron 79:273–279
27. Bu T, Huang Q, Yan L, Huang L, Zhang M, Yang Q, Yang B, Wang J, Zhang D (2018) Ultra technically-simple and sensitive detection for Salmonella Enteritidis by immunochromatographic assay based on gold growth. Food Control 84:536–543
28. Choi DH, Lee SK, Oh YK, Bae BW, Lee SD, Kim S, Shin YB, Kim MG (2010) A dual gold nanoparticle conjugate-based lateral flow assay (LFA) method for the analysis of troponin I. Biosens Bioelectron 25:1999–2002
29. Fang Q, Wang L, Cheng Q, Cai J, Wang Y, Yang M, Hua X, Liu F (2015) A bare-eye based one-step signal amplified semiquantitative immunochromatographic assay for the detection of imidacloprid in Chinese cabbage samples. Anal Chim Acta 881: 82–89
30. Jia CP, Zhong XQ, Hua B, Liu MY, Jing FX, Lou XH, Yao SH, Xiang JQ, Jin QH, Zhao JL (2009) Nano-ELISA for highly sensitive protein detection. Biosens Bioelectron 24:2836–2841
31. Wang Z, Han J, Gao H, Li C, Fu Z (2012) Protein functionalized titania particle as a nanocarrier in a multiple signal antibody amplification strategy for ultrasensitive chemiluminescent immunoassay. Talanta 88:765–768
32. Shi M, Zhao S, Huang Y, Zhao L, Liu YM (2014) Signal amplification in capillary electrophoresis based chemiluminescent immunoassays by using an antibody-gold nanoparticle-DNAzyme assembly. Talanta 124:14–20
33. Zhou Y, Li Y-S, Tian X-L, Zhang Y-Y, Yang L, Zhang J-H, Wang X-R, Lu S-Y, Ren H-L, Liu Z-S (2012) Enhanced ultrasensitive detection of Cr(III) using 5-thio-2-nitrobenzoic acid (TNBA) and horseradish peroxidase (HRP) dually modified gold nanoparticles (AuNPs). Sensors Actuators B Chem 161:1108–1113
34. Lin Y, Xu G, Wei F, Zhang A, Yang J, Hu Q (2016) Detection of CEA in human serum using surface-enhanced Raman spectroscopy coupled with antibody-modified Au and gamma-Fe(2)O(3)@Au nanoparticles. J Pharm Biomed Anal 121:135–140
35. Liu F, Zhang Y, Ge S, Lu J, Yu J, Song X, Liu S (2012) Magnetic graphene nanosheets based electrochemiluminescence immunoassay of cancer biomarker using CdTe quantum dots coated silica nanospheres as labels. Talanta 99:512–519
36. Otieno BA, Krause CE, Latus A, Chikkaveeraiah BV, Faria RC, Rusling JF (2014) On-line protein capture on magnetic beads for ultrasensitive microfluidic immunoassays of cancer biomarkers. Biosens Bioelectron 53:268–274
37. Zhang Y, Yu J (2016) Magnetic materials based immunoassay with improved performance for detection of cancer biomarker. Nanomed Nanotechnol 12:520
38. Kim D, Kim J, Kwak CH, Heo NS, Oh SY, Lee H, Lee G-W, Vilian ATE, Han Y-K, Kim W-S, G-b K, Kwon S, Huh YS (2016) Rapid and label-free bioanalytical method of alpha fetoprotein detection using LSPR chip. J Cryst Growth 469:131–135
39. Lan T, Dong C, Huang X, Ren J (2013) A sensitive, universal and homogeneous method for determination of biomarkers in biofluids by resonance light scattering correlation spectroscopy (RLSCS). Talanta 116:501–507
40. Chen Zong DZ, Yang H, Wang S, Chu M, Li P (2017) Chemiluminescence immunoassay for cardiac troponin T by using silver nanoparticles functionalized with hemin G-quadruplex DNAzyme on a glass chip array. Microchim Acta 184:3197–3204
41. Conzuelo F, Grützke S, Stratmann L, Pingarrón JM, Schuhmann W (2015) Interrogation of immunoassay platforms by SERS and SECM after enzyme-catalyzed deposition of silver nanoparticles. Microchim Acta 183:281–287
42. Li Q, Lv S, Lu M, Lin Z, Tang D (2016) Potentiometric competitive immunoassay for determination of aflatoxin B1 in food by using antibody-labeled gold nanoparticles. Microchim Acta 183: 2815–2822
43. Youhao Zhong YY, Chen Y, Chen W (2016) Gold nanoparticles based lateral flow immunoassay with largely amplified sensitivity for rapid melamine screening. Microchim Acta 183:1989–1994
44. Parolo C, de la Escosura-Muniz A, Merkoci A (2013) Enhanced lateral flow immunoassay using gold nanoparticles loaded with enzymes. Biosens Bioelectron 40:412–416
45. Zhou Y, Tian XL, Li YS, Pan FG, Zhang YY, Zhang JH, Yang L, Wang XR, Ren HL, Lu SY, Li ZH, Chen QJ, Liu ZS, Liu JQ (2011) An enhanced ELISA based on modified colloidal gold nanoparticles for the detection of Pb(II). Biosens Bioelectron 26: 3700–3704
46. Yin H, Zhou Y, Xu Z, Wang M, Ai S (2013) Ultrasensitive electrochemical immunoassay for DNA methyltransferase activity and inhibitor screening based on methyl binding domain protein of MeCP2 and enzymatic signal amplification. Biosens Bioelectron 49:39–45
47. Teng Y, Zhang X, Fu Y, Liu H, Wang Z, Jin L, Zhang W (2011) Optimized ferrocene-functionalized ZnO nanorods for signal amplification in electrochemical immunoassay of Escherichia coli. Biosens Bioelectron 26:4661–4666
48. Cao X, Liu S, Feng Q, Wang N (2013) Silver nanowire-based electrochemical immunoassay for sensing immunoglobulin G with signal amplification using strawberry-like ZnO nanostructures as labels. Biosens Bioelectron 49:256–262
49. Hu W, Chen H, Shi Z, Yu L (2014) Dual signal amplification of surface plasmon resonance imaging for sensitive immunoassay of tumor marker. Anal Biochem 453:16–21
50. Ding L, You J, Kong R, Qu F (2013) Signal amplification strategy for sensitive immunoassay of prostate specific antigen (PSA) based on ferrocene incorporated polystyrene spheres. Anal Chim Acta 793:19–25
51. Wang Y, Li X, Cao W, Li Y, Li H, Du B, Wei Q (2014) Facile fabrication of an ultrasensitive sandwich-type electrochemical immunosensor for the quantitative detection of alpha fetoprotein using multifunctional mesoporous silica as platform and label for signal amplification. Talanta 129:411–416
52. Liu L, Chao Y, Cao W, Wang Y, Luo C, Pang X, Fan D, Wei Q (2014) A label-free amperometric immunosensor for detection of zearalenone based on trimetallic Au-core/AgPt-shell nanorattles and mesoporous carbon. Anal Chim Acta 847:29–36
53. Dong J, Zhao H, Xu M, Ma Q, Ai S (2013) A label-free electrochemical impedance immunosensor based on AuNPs/PAMAM-MWCNT-Chi nanocomposite modified glassy carbon electrode for detection of Salmonella typhimurium in milk. Food Chem 141:1980–1986
54. Lv X, Li Y, Cao W, Yan T, Li Y, Du B, Wei Q (2014) A label-free electrochemiluminescence immunosensor based on silver nanoparticle hybridized mesoporous carbon for the detection of Aflatoxin B1. Sensors Actuators B Chem 202:53–59

55. Feng D, Li L, Zhao J, Zhang Y (2015) Simultaneous electrochemical detection of multiple biomarkers using gold nanoparticles decorated multiwall carbon nanotubes as signal enhancers. Anal Biochem 482:48–54
56. Jiang L, Han J, Li F, Gao J, Li Y, Dong Y, Wei Q (2015) A sandwich-type electrochemical immunosensor based on multiple signal amplification for α-fetoprotein labeled by platinum hybrid multiwalled carbon nanotubes adhered copper oxide. Electrochim Acta 160:7–14
57. Wang J, Yuan R, Chai Y, Cao S, Guan S, Fu P, Min L (2010) A novel immunosensor based on gold nanoparticles and poly-(2,6-pyridinediamine)/multiwall carbon nanotubes composite for immunoassay of human chorionic gonadotrophin. Biochem Eng J 51:95–101
58. Dou X, Zhang L, Liu C, Li Q, Luo J, Yang M (2017) Fluorometric competitive immunoassay for chlorpyrifos using rhodamine-modified gold nanoparticles as a label. Microchim Acta 185:41–48
59. Lingsong Lu BL, Leng J, Wang K, Ma X, Wu S (2016) Electrochemical sandwich immunoassay for human epididymis-specific protein 4 using a screen-printed electrode modified with graphene sheets and gold nanoparticles, and applying a modular magnetic detector device produced by 3D laser sintering. Microchim Acta 183:837–843
60. Liu B, Lu L (2019) Amperometric sandwich immunoassay for determination of myeloperoxidase by using gold nanoparticles encapsulated in graphitized mesoporous carbon. Microchim Acta 186:262–270
61. Zhu F, Zhao G, Dou W (2017) Voltammetric sandwich immunoassay for Cronobacter sakazakii using a screen-printed carbon electrode modified with horseradish peroxidase, reduced graphene oxide, thionine and gold nanoparticles. Microchim Acta 185:45–52
62. Lin J, Zhao Y, Wei Z, Wang W (2011) Chemiluminescence immunoassay based on dual signal amplification strategy of Au/mesoporous silica and multienzyme functionalized mesoporous silica. Mater Sci Eng B 176:1474–1478
63. Zhang X, Guo W, Wang Z, Ke H, Zhao W, Zhang A, Huang C, Jia N (2017) A sandwich electrochemiluminescence immunosensor for highly sensitive detection of alpha fetal protein based on MoS2-PEI-Au nanocomposites and Au@BSA core/shell nanoparticles. Sensors Actuators B Chem 253:470–477
64. Jalal UM, Jin GJ, Eom KS, Kim MH, Shim JS (2018) On-chip signal amplification of magnetic bead-based immunoassay by aviating magnetic bead chains. Bioelectrochemistry 122:221–226
65. Wang X, Gao P, Yan T, Li R, Xu R, Zhang Y, Du B, Wei Q (2018) Ultrasensitive photoelectrochemical immunosensor for insulin detection based on dual inhibition effect of CuS-SiO2 composite on CdS sensitized C-TiO2. Sensors Actuators B Chem 258:1–9
66. Bogdanovic J, Colon J, Baker C, Huo Q (2010) A label-free nanoparticle aggregation assay for protein complex/aggregate detection and study. Anal Biochem 405:96–102
67. Du B, Li Z, Cheng Y (2008) Homogeneous immunoassay based on aggregation of antibody-functionalized gold nanoparticles coupled with light scattering detection. Talanta 75:959–964
68. Li YS, Zhou Y, Meng XY, Zhang YY, Song F, Lu SY, Ren HL, Hu P, Liu ZS, Zhang JH (2014) Gold nanoparticle aggregation-based colorimetric assay for beta-casein detection in bovine milk samples. Food Chem 162:22–26
69. Huo Q (2010) Protein complexes/aggregates as potential cancer biomarkers revealed by a nanoparticle aggregation immunoassay. Colloids Surf B: Biointerfaces 78:259–265
70. Wang X, Li Y, Quan D, Wang J, Zhang Y, Du J, Peng J, Fu Q, Zhou Y, Jia S, Wang Y, Zhan L (2012) Detection of hepatitis B surface antigen by target-induced aggregation monitored by dynamic light scattering. Anal Biochem 428:119–125
71. Liang Y, Huang X, Chen X, Zhang W, Ping G, Xiong Y (2018) Plasmonic ELISA for naked-eye detection of ochratoxin A based on the tyramine-H 2 O 2 amplification system. Sensors Actuators B Chem 259:162–169
72. Nie XM, Huang R, Dong CX, Tang LJ, Gui R, Jiang JH (2014) Plasmonic ELISA for the ultrasensitive detection of Treponema pallidum. Biosens Bioelectron 58:314–319
73. Wang J, Lu J, Su S, Gao J, Huang Q, Wang L, Huang W, Zuo X (2015) Binding-induced collapse of DNA nano-assembly for naked-eye detection of ATP with plasmonic gold nanoparticles. Biosens Bioelectron 65:171–175
74. Zhang J, He L, Zhang X, Wang J, Yang L, Liu B, Jiang C, Zhang Z (2017) Colorimetric and SERS dual-readout for assaying alkaline phosphatase activity by ascorbic acid induced aggregation of Ag coated Au nanoparticles. Sensors Actuators B Chem 253:839–845
75. de la Rica R, Stevens MM (2012) Plasmonic ELISA for the ultrasensitive detection of disease biomarkers with the naked eye. Nat Nanotechnol 7:821–824
76. Panferov VG, Safenkova IV, Zherdev AV, Dzantiev BB (2018) Post-assay growth of gold nanoparticles as a tool for highly sensitive lateral flow immunoassay. Application to the detection of potato virus X. Microchim Acta 185:506–513
77. Yao C, Yu S, Li X, Wu Z, Liang J, Fu Q, Xiao W, Jiang T, Tang Y (2017) A plasmonic ELISA for the naked-eye detection of chromium ions in water samples. Anal Bioanal Chem 409:1093–1100
78. Liang J, Yao C, Li X, Wu Z, Huang C, Fu Q, Lan C, Cao D, Tang Y (2015) Silver nanoprism etching-based plasmonic ELISA for the high sensitive detection of prostate-specific antigen. Biosens Bioelectron 69:128–134
79. Xuan Z, Li M, Rong P, Wang W, Li Y, Liu D (2016) Plasmonic ELISA based on the controlled growth of silver nanoparticles. Nanoscale 8:17271–17277
80. Liu D, Yang J, Wang HF, Wang Z, Huang X, Wang Z, Niu G, Hight Walker AR, Chen X (2014) Glucose oxidase-catalyzed growth of gold nanoparticles enables quantitative detection of attomolar cancer biomarkers. Anal Chem 86:5800–5806
81. Huang H, Zhou Y, Zhao Q, Zhang L, Liu L, Xia X, Yi S (2017) A highly sensitive EDTA-based senor for detection of disease biomarker and drug. Sensors Actuators B Chem 249:478–485
82. Wei H, Wang E (2013) Nanomaterials with enzyme-like characteristics (nanozymes): next-generation artificial enzymes. Chem Soc Rev 42:6060–6093
83. Lan D, Li B, Zhang Z (2008) Chemiluminescence flow biosensor for glucose based on gold nanoparticle-enhanced activities of glucose oxidase and horseradish peroxidase. Biosens Bioelectron 24:940–944
84. Jv Y, Li B, Cao R (2010) Positively-charged gold nanoparticles as peroxidase mimic and their application in hydrogen peroxide and glucose detection. Chem Commun (Camb) 46:8017–8019
85. Das J, Kim H, Jo K, Park KH, Jon S, Lee K, Yang H (2009) Fast catalytic and electrocatalytic oxidation of sodium borohydride on palladium nanoparticles and its application to ultrasensitive DNA detection. Chem Commun (Camb):6394–6396
86. Liu Y, Wang J, Song X, Xu K, Chen H, Zhao C, Li J (2018) Colorimetric immunoassay for Listeria monocytogenes by using core gold nanoparticles, silver nanoclusters as oxidase mimetics, and aptamer-conjugated magnetic nanoparticles. Microchim Acta 185:360–366
87. Syed Rahin Ahmed JK, Suzuki T, Lee J, Park EY (2016) Detection of Influenza Virus Using Peroxidase-Mimic of Gold Nanoparticles. Biotechnol Bioeng 113:2298–2303
88. de la Escosura-Muniz A, Maltez-da Costa M, Merkoci A (2009) Controlling the electrochemical deposition of silver onto gold nanoparticles: reducing interferences and increasing the sensitivity of magnetoimmuno assays. Biosens Bioelectron 24:2475–2482

89. Chen G, Jin M, Yan M, Cui X, Wang Y, Zheng W, Qin G, Zhang Y, Li M, Liao Y, Zhang X, Yan F, Abd El-Aty AM, Hacimuftuoglu A, Wang J (2019) Colorimetric bio-barcode immunoassay for parathion based on amplification by using platinum nanoparticles acting as a nanozyme. Microchim Acta 186:339–348
90. Gao L, Zhuang J, Nie L, Zhang J, Zhang Y, Gu N, Wang T, Feng J, Yang D, Perrett S, Yan X (2007) Intrinsic peroxidase-like activity of ferromagnetic nanoparticles. Nat Nanotechnol 2:577–583
91. Duan D, Fan K, Zhang D, Tan S, Liang M, Liu Y, Zhang J, Zhang P, Liu W, Qiu X, Kobinger GP, Gao GF, Yan X (2015) Nanozyme-strip for rapid local diagnosis of Ebola. Biosens Bioelectron 74: 134–141
92. Ahmed SR, Takemeura K, Li TC, Kitamoto N, Tanaka T, Suzuki T, Park EY (2017) Size-controlled preparation of peroxidase-like graphene-gold nanoparticle hybrids for the visible detection of norovirus-like particles. Biosens Bioelectron 87:558–565
93. Ahmed SR, Kim J, Suzuki T, Lee J, Park EY (2016) Enhanced catalytic activity of gold nanoparticle-carbon nanotube hybrids for influenza virus detection. Biosens Bioelectron 85:503–508
94. Wang H, Li S, Si Y, Zhang N, Sun Z, Wu H, Lin Y (2014) Platinum nanocatalysts loaded on graphene oxide-dispersed carbon nanotubes with greatly enhanced peroxidase-like catalysis and electrocatalysis activities. Nanoscale 6:8107–8116
95. Wang GL, Shu JX, Dong YM, Wu XM, Li ZJ (2015) An ultrasensitive and universal photoelectrochemical immunoassay based on enzyme mimetics enhanced signal amplification. Biosens Bioelectron 66:283–289
96. Sun Z, Wang W, Wen H, Gan C, Lei H, Liu Y (2015) Sensitive electrochemical immunoassay for chlorpyrifos by using flake-like Fe3O4 modified carbon nanotubes as the enhanced multienzyme label. Anal Chim Acta 899:91–99
97. Lin M, Liu Y, Sun Z, Zhang S, Yang Z, Ni C (2012) Electrochemical immunoassay of benzo[a]pyrene based on dual amplification strategy of electron-accelerated Fe3O4/polyaniline platform and multi-enzyme-functionalized carbon sphere label. Anal Chim Acta 722:100–106
98. Wu D, Fan H, Li Y, Zhang Y, Liang H, Wei Q (2013) Ultrasensitive electrochemical immunoassay for squamous cell carcinoma antigen using dumbbell-like Pt-Fe(3)O(4) nanoparticles as signal amplification. Biosens Bioelectron 46:91–96
99. Ahmed SR, Kim J, Suzuki T, Lee J, Park EY (2016) Detection of influenza virus using peroxidase-mimic of gold nanoparticles. Biotechnol Bioeng 113:2298–2303
100. Wei Q, Xin X, Du B, Wu D, Han Y, Zhao Y, Cai Y, Li R, Yang M, Li H (2010) Electrochemical immunosensor for norethisterone based on signal amplification strategy of graphene sheets and multienzyme functionalized mesoporous silica nanoparticles. Biosens Bioelectron 26:723–729
101. Bu SJ, Wang KY, Bai HS, Leng Y, Ju CJ, Wang CY, Liu WS, Wan JY (2019) Immunoassay for pathogenic bacteria using platinum nanoparticles and a hand-held hydrogen detector as transducer. Application to the detection of Escherichia coli O157:H7. Microchim Acta 186:296–302
102. Liu F, Zhang Y, Yu J, Wang S, Ge S, Song X (2014) Application of ZnO/graphene and S6 aptamers for sensitive photoelectrochemical detection of SK-BR-3 breast cancer cells based on a disposable indium tin oxide device. Biosens Bioelectron 51:413–420
103. Norouzi P, Gupta VK, Faridbod F, Pirali-Hamedani M, Larijani B, Ganjali MR (2011) Carcinoembryonic antigen admittance biosensor based on Au and ZnO nanoparticles using FFT admittance voltammetry. Anal Chem 83:1564–1570
104. Wang D, Gan N, Zhou J, Xiong P, Cao Y, Li T, Pan D, Jiang S (2014) Signal amplification for multianalyte electrochemical immunoassay with bidirectional stripping voltammetry using metal-enriched polymer nanolabels. Sensors Actuators B Chem 197: 244–253
105. Su H, Yuan R, Chai Y, Mao L, Zhuo Y (2011) Ferrocenemonocarboxylic-HRP@Pt nanoparticles labeled RCA for multiple amplification of electro-immunosensing. Biosens Bioelectron 26:4601–4604
106. Tang J, Tang D, Li Q, Su B, Qiu B, Chen G (2011) Sensitive electrochemical immunoassay of carcinoembryonic antigen with signal dual-amplification using glucose oxidase and an artificial catalase. Anal Chim Acta 697:16–22
107. Li NL, Jia LP, Ma RN, Jia WL, Lu YY, Shi SS, Wang HS (2017) A novel sandwiched electrochemiluminescence immunosensor for the detection of carcinoembryonic antigen based on carbon quantum dots and signal amplification. Biosens Bioelectron 89:453–460
108. Lan F, Sun G, Liang L, Ge S, Yan M, Yu J (2016) Microfluidic paper-based analytical device for photoelectrochemical immunoassay with multiplex signal amplification using multibranched hybridization chain reaction and PdAu enzyme mimetics. Biosens Bioelectron 79:416–422
109. Zang S, Liu YJ, Lin MH, Kang JL, Sun YM, Lei HT (2013) A dual amplified electrochemical immunosensor for ofloxacin: Polypyrrole film-Au nanocluster as the matrix and multi-enzyme-antibody functionalized gold nanorod as the label. Electrochim Acta 90:246–253
110. Huang T, Meng Q, Jie G (2015) Silver nanowires-based signal amplification for CdSe quantum dots electrochemiluminescence immunoassay. Biosens Bioelectron 66:84–88
111. Fan GC, Ren XL, Zhu C, Zhang JR, Zhu JJ (2014) A new signal amplification strategy of photoelectrochemical immunoassay for highly sensitive interleukin-6 detection based on TiO2/CdS/CdSe dual co-sensitized structure. Biosens Bioelectron 59:45–53
112. Rong Z, Wang C, Wang J, Wang D, Xiao R, Wang S (2016) Magnetic immunoassay for cancer biomarker detection based on surface-enhanced resonance Raman scattering from coupled plasmonic nanostructures. Biosens Bioelectron 84:15–21
113. Zhan L, Wu WB, Yang L, Huang CZ (2017) Sensitive detection of respiratory syncytial virus based on a dual signal amplified plasmonic enzyme-linked immunosorbent assay. Anal Chim Acta 962:73–79
114. Zhang J, Xiong Z, Chen Z (2017) Ultrasensitive electrochemical microcystin-LR immunosensor using gold nanoparticle functional polypyrrole microsphere catalyzed silver deposition for signal amplification. Sensors Actuators B Chem 246:623–630
115. Li S, Luo J, Yang X, Wan Y, Liu C (2014) A novel immunosensor for squamous cell carcinoma antigen determination based on CdTe@Carbon dots nanocomposite electrochemiluminescence resonance energy transfer. Sensors Actuators B Chem 197:43–49
116. Li L, Feng D, Zhang Y (2016) Simultaneous detection of two tumor markers using silver and gold nanoparticles decorated carbon nanospheres as labels. Anal Biochem 505:59–65
117. Liu F, Deng W, Zhang Y, Ge S, Yu J, Song X (2014) Application of ZnO quantum dots dotted carbon nanotube for sensitive electrochemiluminescence immunoassay based on simply electrochemical reduced Pt/Au alloy and a disposable device. Anal Chim Acta 818:46–53
118. Yang H, Sun G, Zhang L, Zhang Y, Song X, Yu J, Ge S (2016) Ultrasensitive photoelectrochemical immunoassay based on CdS@Cu 2 O co-sensitized porous ZnO nanosheets and promoted by multiwalled carbon nanotubes. Sensors Actuators B Chem 234: 658–666
119. Yang J, Shen H, Zhang X, Tao Y, Xiang H, Xie G (2016) A novel platform for high sensitivity determination of PbP2a based on gold nanoparticles composited graphitized mesoporous carbon and doxorubicin loaded hollow gold nanospheres. Biosens Bioelectron 77:1119–1125
120. Tiantian Dong QT, Zhao K, Deng A, Li J (2017) Ultrasensitive electrochemiluminescent salbutamol immunoassay with dual-

signal amplification using CdSe@SiO2 as label and gold nanoparticles as substrate. Microchim Acta 184:961–968
121. Du P, Jin M, Chen G, Zhang C, Cui X, Zhang Y, Zhang Y, Zou P, Jiang Z, Cao X, She Y, Jin F, Wang J (2017) Competitive colorimetric triazophos immunoassay employing magnetic microspheres and multi-labeled gold nanoparticles along with enzymatic signal enhancement. Microchim Acta 184:3705–3712
122. Gou D, Xie G, Li Y, Zhang X, Chen H (2018) Voltammetric immunoassay for Mycobacterium tuberculosis secretory protein MPT64 based on a synergistic amplification strategy using rolling circle amplification and a gold electrode modified with graphene oxide, Fe3O4 and Pt nanoparticles. Microchim Acta 185:436–444
123. Hu L, Dong T, Zhao K, Deng A, Li J (2017) Ultrasensitive electrochemiluminescent brombuterol immunoassay by applying a multiple signal amplification strategy based on a PAMAM-gold nanoparticle conjugate as the bioprobe and Ag@Au core shell nanoparticles as a substrate. Microchim Acta 184:3415–3423
124. Liu J, Shang Y, Zhu Q, Zhang X, Zheng J (2019) A voltammetric immunoassay for the carcinoembryonic antigen using silver(I)-terephthalate metal-organic frameworks containing gold nanoparticles as a signal probe. Microchim Acta 186:509–516
125. Mars A, Ben Jaafar S, Gaied ABA, Raouafi N (2018) Electrochemical immunoassay for lactalbumin based on the use of ferrocene-modified gold nanoparticles and lysozyme-modified magnetic beads. Microchim Acta 185:449–456
126. Miao L, Jiao L, Zhang J, Li H (2016) Amperometric sandwich immunoassay for the carcinoembryonic antigen using a glassy carbon electrode modified with iridium nanoparticles, polydopamine and reduced graphene oxide. Microchim Acta 184:169–175
127. Singal S, Srivastava AK, Gahtori B, Rajesh (2016) Immunoassay for troponin I using a glassy carbon electrode modified with a hybrid film consisting of graphene and multiwalled carbon nanotubes and decorated with platinum nanoparticles. Microchim Acta 183:1375–1384
128. Wang H, Ma Z (2017) Amperometric immunoassay for the tumor marker neuron-specific enolase using a glassy carbon electrode modified with a nanocomposite consisting of polyresorcinol and of gold and platinum nanoparticles. Microchim Acta 184:3247–3253
129. You H, Hua X, Feng L, Sun N, Rui Q, Wang L, Wang M (2017) Competitive immunoassay for imidaclothiz using upconversion nanoparticles and gold nanoparticles as labels. Microchim Acta 184:1085–1092
130. Peng D, Liang R-P, Huang H, Qiu J-D (2016) Electrochemical immunosensor for carcinoembryonic antigen based on signal amplification strategy of graphene and Fe3O4/Au NPs. J Electroanal Chem 761:112–117
131. Huang X, Chen R, Xu H, Lai W, Xiong Y (2016) Nanospherical Brush as Catalase Container for Enhancing the Detection Sensitivity of Competitive Plasmonic ELISA. Anal Chem 88: 1951–1958
132. Zhang Z, Zhu N, Dong S, Huang M, Yang L, Wu X, Liu Z, Jiang J, Zou Y (2017) Plasmonic ELISA Based on Nanospherical Brush-Induced Signal Amplification for the Ultrasensitive Naked-Eye Simultaneous Detection of the Typical Tetrabromobisphenol A Derivative and Byproduct. J Agric Food Chem 66:2996–3002
133. De Wang NG, Zhou J, Xiong P, Cao Y, Li T, Pan D, Jiang S (2014) Signal amplification for multianalyte electrochemical immunoassay with bidirectional stripping voltammetry using metal-enriched polymer nanolabels. Sensors Actuators B Chem 197:244–253
134. Dong Peng R-PL, He H, Qiu J-D (2016) Electrochemical immunosensor for carcinoembryonic antigen based on signal amplification strategy of graphene and Fe3O4/Au NPs. J Electroanal Chem 761:112–117
135. Gao-Chao Fan X-LR, Cheng Z, Zhang J-R, Zhu J-J (2014) A new signal amplification strategy of photoelectrochemical immunoassay for highly sensitive interleukin-6 detection based on TiO2/CdS/CdSe dual co-sensitized structure. Biosens Bioelectron 59:45–53
136. Huang X, Chen R, Xu H, Lai W, Xiong Y (2016) Nanospherical Brush as Catalase Container for Enhancing the Detection Sensitivity of Competitive Plasmonic ELISA. Anal Chem 88: 1951–1958
137. Huilan Su RY, Chai Y, Mao L, Zhuo Y (2011) Ferrocenemonocarboxylic-HRP@Pt nanoparticles labeled RCA for multiple amplification of electro-immunosensing. Biosens Bioelectron 26:4601–4604
138. Lan F, Sun G, Liang L, Ge S, Yan M, Yu J (2016) Microfluidic paper-based analytical device for photoelectrochemical immunoassay with multiplex signal amplification using multibranched hybridization chain reaction and PdAu enzyme mimetics. Biosens Bioelectron 79:416–422
139. Li L, Feng D, Zhang Y (2016) Simultaneous detection of two tumor markers using silver and gold nanoparticles decorated carbon nanospheres as labels. Anal Biochem 505:59–65
140. Liu F, Zhang Y, Yu J, Wang S, Ge S, Song X (2014) Application of ZnO/graphene and S6 aptamers for sensitive photoelectrochemical detection of SK-BR-3 breast cancer cells based on a disposable indium tin oxide device. Biosens Bioelectron 51:413–420
141. Rong Z, Wang C, Wang J, Wang D, Xiao R, Wang S (2016) Magnetic immunoassay for cancer biomarker detection based on surface-enhanced resonance Raman scattering from coupled plasmonic nanostructures. Biosens Bioelectron 84:15–21
142. Shuhuai Li JL, Yang X, Wan Y, Liu C (2014) A novel immunosensor for squamous cell carcinoma antigen determination based on CdTe@Carbon dots. Sensors Actuators B Chem 197:43–49
143. Tang J, Tang D, Li Q, Su B, Qiu B, Chen G (2011) Sensitive electrochemical immunoassay of carcinoembryonic antigen with signal dual-amplification using glucose oxidase and an artificial catalase. Anal Chim Acta 697:16–22
144. Xinle Jia XC, Han J, Ma J, Ma Z (2014) Triple signal amplification using gold nanoparticles, bienzyme and platinum nanoparticles functionalized graphene as enhancers for simultaneous multiple electrochemical immunoassay. Biosens Bioelectron 53:65–70
145. Yang J, Shen H, Zhang X, Tao Y, Xiang H, Xie G (2016) A novel platform for high sensitivity determination of PbP2a based on gold nanoparticles composited graphitized mesoporous carbon and doxorubicin loaded hollow gold nanospheres. Biosens Bioelectron 77:1119–1125
146. Zhan L, Wu WB, Yang L, Huang CZ (2017) Sensitive detection of respiratory syncytial virus based on a dual signal amplified plasmonic enzyme-linked immunosorbent assay. Anal Chim Acta 962:73–79
147. Zhang Z, Zhu N, Dong S, Huang M, Yang L, Wu X, Liu Z, Jiang J, Zou Y (2018) Plasmonic ELISA Based on Nanospherical Brush-Induced Signal Amplification for the Ultrasensitive Naked-Eye Simultaneous Detection of the Typical Tetrabromobisphenol A Derivative and Byproduct. J Agric Food Chem 66:2996–3002